Analysis of Millimeter-Wave Multi-Hop Networks with Full-Duplex Buffered Relays

Guang Yang, *Student Member, IEEE*, Ming Xiao, *Senior Member, IEEE*, Hussein Al-Zubaidy, *Senior Member, IEEE*, Yongming Huang, *Senior Member, IEEE*, and James Gross, *Senior Member, IEEE*

***Abstract*—The abundance of spectrum in the millimeter-wave (mmWave) bands makes it an attractive alternative for future wireless communication systems. Such systems are expected to provide data transmission rates in the order of multi-gigabits per second in order to satisfy the ever-increasing demand for high rate data communication. Unfortunately, mmWave radio is subject to severe path loss which limits its usability for long-range outdoor communication. In this work, we propose a multi-hop mmWave wireless network for outdoor communication where multiple full-duplex buffered relays are used to extend the communication range, while providing end-to-end performance guarantees to the traffic traversing the network. We provide a cumulative service process characterization for the mmWave propagation channel with self-interference in terms of the moment generating function (MGF) of its channel capacity. We then use this characterization to compute probabilistic upper bounds on the overall network performance, i.e., total backlog and end-to-end delay. Furthermore, we study the effect of self-interference on the network performance and propose an optimal power allocation scheme to mitigate its impact in order to enhance network performance. Finally, we investigate the relation between relay density and network performance under a sum power constraint. We show that increasing relay density may have adverse effects on network performance, unless the self-interference can be kept sufficiently small.**

***Index Terms*—Millimeter-wave; Multi-hop; Moment Generating Functions; Delay; Backlog.**

I. Introduction

With rapidly increasing demands on network service, wireless communications in millimeter-wave (mmWave) bands (ranging from 24.25 GHz to 300 GHz) becomes a promising technology to improve the network throughput for future communication systems [1]. Compared to conventional wireless communications in lower frequency bands, i.e., sub 6 GHz, mmWave wireless communications have significant advantages, including considerably broader bandwidth, lower cost electronics, and higher gain directional antenna implementations [2]. These attributes make mmWave a promising solution for the wireless backhaul [3], since the initial cost of fiber optic backhaul tends to be quite high and the conventional microwave based backhaul networks cannot support the throughput requirements of future networks.

This work was supported partly by National Natural Science Foundation of China under Grant 61371105, National 973 Programs 2013CB329001 and EU Marie Curie Project, QUICK, No. 612652.

G. Yang, M. Xiao, J. Gross, and H. Al-Zubaidy are with the Communication Theory Department, KTH Royal Institute of Technology, Stockholm, Sweden (Email: {gy, mingx, hzubaidy}@kth.se, james.gross@ee.kth.se).

Y. Huang is with the School of Information Science and Engineering, Southeast University, Nanjing 210096, China (Email: huangym@seu.edu.cn).

The mmWave technology can be utilized for both indoor and outdoor communications. A significant amount of experimental results for investigating the indoor mmWave wireless personal area networks (WPAN) were reported in recent years [4]–[8]. For outdoor environments, in [9], antennas with narrow beamwidth were used to measure the path loss in urban street environments for the line-of-sight (LOS) and non-line-of-sight (NLOS) scenarios. In [10], a channel sounder was deployed to estimate the outdoor 60 GHz channel using a 59 GHz horn antenna. Results show that the path loss exponent for the 60 GHz channel is between 2 and 2.5 for the outdoor environment, such as airport fields, urban streets or tunnels. In the recent work [11], the spatial statistical models of mmWave channels at 28 GHz and 73 GHz were established based on real-world urban measurements. Also, the small-scale fading effects were shown to be negligible in mmWave bands due to the short wavelength [6], [12]. Hence, the channel fading is dominated by the shadowing effect, which is generally modeled as a log-normal random variable.

In light of the above, it is clear that, the use of mmWave bands is limited to short-distance LOS communications, e.g., usually below 500 meters. To overcome larger distances or obstructed paths, especially in outdoor applications for high data rate transmissions, a strategically placed store-and-forward relay node may be used to form a multi-hop wireless network. Thus, it is our claim that multi-hop communications can be utilized to mitigate the effects of path loss over long distances and/or the effect of NLOS, while maintaining the traffic flows' quality of service (QoS) requirements. In this case, an understanding of corresponding network performance in terms of end-to-end delay and loss probability becomes the key to support real-time missions and critical applications, e.g., online banking, remote health, transportation systems operation and control, and electric power systems. Nevertheless, an analytical model for the multi-hop network in mmWave bands does not exist, and its performance is not yet understood.

To improve the network throughput significantly, the full-duplex relaying technique recently has drawn tremendous attention [13]. An full-duplex relay can perform simultaneous signal reception and transmission, thereby providing a better performance in terms of spectral efficiency than its half-duplex counterpart. However, it suffers self-interferences at the receiver from its transmitter. Despite that the presence of self-interference inevitably deteriorates the system performance, the loss can be largely mitigated through the use of effective interference cancellation techniques [14], [15]. In recent year, thanks to the advances in self-interference

cancellation techniques and hardware designs, the application of full-duplex relays emerges in mmWave communications. In [16], [17], it is shown that, the self-interference cancellation amount can be achieved up to $80 \sim 100$ dB via passive suppression, analog cancellation, and digital cancellation. In [18], the energy efficiency of mmWave full-duplex relaying system was comprehensively investigated. Numerous efforts dedicated to the study of full-duplex relaying for mmWave applications can be found in [19]–[21].

In this work, we provide a probabilistic end-to-end delay and backlog analysis of such networks in terms of the underlying channel parameters. This analysis can be used as a guideline for planning and operating QoS-driven multi-hop mmWave network. The analysis of multi-hop wireless networks in mmWave bands poses two main challenges: (i) the service process characterization for mmWave fading channel, and (ii) multi-hop network performance analysis. The first challenge comes from the random nature of the mmWave fading channel which results in time varying channel capacity, and the second challenge is a direct result of the limitations and strict assumptions of the traditional queuing theory, which is the main tool for network analysis, when applied to queuing networks. To address these two challenges, we adopt a moment generating function (MGF)-based stochastic network calculus approach [22] for the analysis of networks of tandem queues. Then the service process, which is a function of the instantaneous channel capacity, is given in terms of the MGF of the fading channel distribution. This addresses the first challenge. Furthermore, we utilize network calculus to address the second challenge by using the service concatenation property.

A. Methodologies for Wireless Network Analysis

Network calculus is an effective methodology for network performance analysis. It was originally proposed by Cruz [23], [24] in the early 90's for the worst-case analysis of deterministic networked systems. Since then, the methodology has been extended to probabilistic settings. Following the pioneering works in [25]–[27] on MGF-based traffic and service characterization, in order to model traffic and service processes with independent increments and to utilize independence among multiplexed flows, the moment generating function (MGF) based network calculus was proposed [22]. Typically, the MGF approach to network calculus employs a finite-state Markov channel abstraction for the analysis of wireless fading channels [28], [29]. It is worth noting that MGF-based approach was used, outside the network calculus framework, for the analysis of various fading channels and relaying channels, e.g., [30]–[33]. In contrast, the $(\min, \times)$ network calculus approach, proposed by [34], provides probabilistic performance bounds directly in terms of the fading channel parameters. It does that by transferring the problem from the 'bit domain,' where traffic and service quantities are measured in bits, to the 'SNR domain,' where these quantities are described by their SNR equivalence when measured at the channel capacity limit, using the exponential function. To apply the $(\min, \times)$ network calculus to non-identically distributed multi-hop wireless networks, a recursive formula for delay bound computation was developed in [35].

To evaluate the performance of our proposed mmWave multi-hop wireless network, we model a multi-hop path in the network by a tandem of queues with service processes that represent the time-varying service offered by the underlying mmWave channel. Then we follow an MGF-based network calculus approach to compute probabilistic end-to-end delay and backlog bounds for that network. Without loss of generality, we use a self-interference coefficient, which is a discounting parameter for the service offered by the channel, to characterize the interference at each relaying transceiver.

B. Motivations and Contributions

Although network calculus has been around for some years, its application to wireless networks analysis is fairly recent. Furthermore, in the existing related work, the self-interference factor was not taken into account. To our best knowledge, the performance guarantees of mmWave multi-hop wireless networks considering self-interfered channels have not yet been addressed. Coupled with the importance of mmWave networks for the next generation mobile communications, it motivates us to investigate the backlog and delay performance, as well as the constrained sum power budget and QoS trade-off corresponding to the self-interfered channel.

As aforementioned, there exist two major difficulties for our study. More exactly, the $(\min, \times)$-based wireless network calculus presented in [34] is not feasible to analyze mmWave networks. This is because, the prerequisite for applying $(\min, \times)$ algebra is the existence of Mellin transform for stochastic processes. However, in mmWave communications, the large-scaling fading, i.e., shadowing effect following the log-normal distribution, plays a dominant role, and the resulting SNR has no corresponding Mellin transform. Thus, an alternative solution is required to circumvent this intractability. In addition, regarding the multi-hop performance analysis, the difficulty mainly lies in generally analyzing the end-to-end performance guarantees in wide-sense heterogeneous networks, i.e., the fading characteristics of distinct channels may be different or identical. In most of previous studies, homogeneous fading channels are commonly assumed for multi-hop networks. In the recent work [35], the heterogeneous network was investigated, and a recursive way for obtaining the network service curve was explored. As the number of hops increases, the complexity of recursive method linearly grows. Thus, a straightforward method may effectively reduce the complexity, especially when the network size goes large.

Based on the motivation and specific challenges above, the main contributions of this paper are two-fold: (i) contribution to the theory of network calculus that is represented by a simplified closed-form expression for the network service curve applicable to both homogeneous and heterogeneous wireless networks, and (ii) contribution to the application by providing a service process characterization for mmWave fading channels with self-interference, in terms of the MGF of the fading distribution. More precisely, first, we devise a straightforward method to compute the network service curve, which is generally applicable for both homogeneous and heterogeneous multi-hop networks, such that the service

characterization can be formulated in an efficient and unified manner. Second, to address the problem in obtaining the Mellin transform associated with specific fading distributions of mmWave channels, we alternatively derived a parameterized upper bound for the actual MGF of network service curve. The proposed bound, which is actually a heuristic method to keep track of service processes, can be utilized for a broad class of fading distributions in that the Mellin transform for SNR cannot apply, not limited to the log-normal fading in this paper. Additional contributions of this work include

- An optimal power allocation scheme, based on the proposed methodology, more precisely, for mmWave multi-hop networks with independent and identically distributed (i.i.d.) shadowing under end-to-end delay constraint.
- The insight that, under optimal power allocation, the end-to-end performance bounds exponentially degrade with the self-interference coefficient. This suggests that managing self-interference can be extremely rewarding.

Our work builds on own previous work [36], where a service characterization for a single-hop 60 GHz system without self interference was presented.

The remainder of the paper is organized as follows. In Sec. II, we provide the basics for MGF-based stochastic network calculus. We construct a model for the mmWave multi-hop network and derive its probabilistic backlog and delay bounds in Sec. III. In Sec. IV we propose an optimal power allocation strategy that results in better performance bounds. An asymptotic performance analysis of the network with self-interference is presented in Sec. V. Numerical results and simulations are presented in Sec. VI, where we discuss the validity and the effectiveness of our analytical upper bounds and investigate the impacts of self-interference coefficient and relay density on network performance. Conclusions are presented in Sec. VII.

II. Preliminaries

In this section we mainly provide a brief review of network calculus fundamental results and the MGF-based stochastic network calculus framework in particular. Due to space limitation, we will not elaborate proofs for the presented fundamental results. For better understanding of network calculus theory, more related details can be in [25], [28], [37]–[39].

A. Model and Notation

Assuming a fluid-flow, discrete-time queuing system with a buffer of infinite size, and given a time interval $[s,t)$, $0 \leq s \leq t$, we define the non-decreasing (in t) bivariate processes $A(s,t), D(s,t)$ and $S(s,t)$ as the cumulative arrival to, departure from and service offered by the system as shown in Fig. 1. We further assume that A, D and S are stationary non-negative random processes with $A(t,t) = D(t,t) = S(t,t) = 0$ for all $t \geq 0$. The cumulative arrival and service processes are given in terms of their instantaneous values during the i^{th} time slot, a_i and s_i respectively, as follows

$$A(s,t) = \sum_{k=s}^{t-1} a_i \quad \text{and} \quad S(s,t) = \sum_{k=s}^{t-1} s_i \,, \tag{1}$$

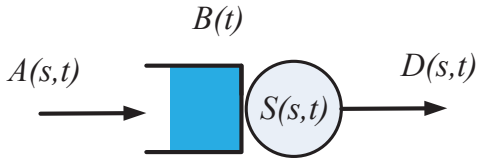

Fig. 1. A queuing model for a store-and-forward node.

for all $0 \leq s \leq t$. We assume that time slots are normalized to 1 time unit. We denote by $B(t)$ the backlog (the amount of buffered data) at time t. Furthermore, $W(t)$ denotes the virtual delay of the system at time t.

Network calculus is based on $(\min,+)$-algebra, for which in particular the convolution and deconvolution are important to obtain bounds on the system performance. More precisely, given the non-decreasing and strictly positive bivariate processes $X(s,t)$ and $Y(s,t)$, the $(\min,+)$ convolution and deconvolution are respectively defined as

$$(X \otimes Y)(s,t) \triangleq \inf_{s \leq \tau \leq t} \{X(s,\tau) + Y(\tau,t)\}$$

and

$$(X \oslash Y)(s,t) \triangleq \sup_{0 \leq \tau \leq s} \{X(\tau,t) - Y(\tau,s)\}.$$

B. Network Calculus Basics

In network calculus, the queuing system in Fig. 1 is analyzed with the arrival process $A(s,t)$ as input and the departure process $D(s,t)$ as system output. Input and output are related to each through the $(\min,+)$ convolution of the input with the service process $S(s,t)$. In particular, we consider in the following time varying systems known as *dynamic servers*, for which for all $t \geq 0$ the network element offers a time varying service S that satisfies the following input-output inequality [25] $D(0,t) \geq (A \otimes S)(0,t)$, which holds with strict equality when the system is linear [38]. One typical example is a work-conserving link with a time-variant capacity, with the available service $S(s,t)$ during interval $[s,t)$.

Based on this server model, the total backlog and end-to-end delay, which are critical measures in system evaluation, can be studied via network calculus. On one hand, buffer dimensioning is a major factor to consider when designing and implementing broadband networks. This is true due to the space restriction and cost of storage in intermediate network devices, e.g., routers in high data rate networks. On the other hand, end-to-end delay is closely related to the quality of service (QoS) and user experience for many networked applications, e.g., voice and video services. For a given queuing system with cumulative arrival $A(0,t)$ and departure $D(0,t)$ and for $t \geq 0$, the backlog at time t, $B(t)$ is defined as the amount of traffic remaining in the system by time t. Therefore,

$$B(t) \triangleq A(0,t) - D(0,t)\,. \tag{2}$$

Likewise, the virtual delay $W(t)$ is defined as the time it takes the last bit received by time t to depart the system under a first-come-first-serve (FCFS) scheduling regime. Hence,

$$W(t) \triangleq \inf\{w \geq 0 : A(0,t) \leq D(0,t+w)\}. \tag{3}$$

Substituting $D(0,t) \geq (A \otimes S)(0,t)$ in the above expressions and after some manipulation and using definitions of $(\min,+)$ convolution and deconvolution, we can obtain the following bounds on $B(t)$ and $W(t)$ respectively, as

$$B(t) \leq (A \oslash S)(t,t) \tag{4}$$

and

$$W(t) \leq \inf\{w \geq 0 : (A \oslash S)(t+w,t) \leq 0\}. \tag{5}$$

A main attribute of network calculus is its ability to handle concatenated systems, e.g., multi-hop store-and-forward networks. This is mainly achieved using the server concatenation theory, which states that a network service process can be computed as the $(\min,+)$ convolution of the individual nodes' service processes [38]. More precisely, given n tandem servers, the network service process $S_{\text{net}}(s,t)$ is given by

$$S_{\text{net}}(s,t) = (S_1 \otimes S_2 \otimes \cdots \otimes S_n)(s,t), \tag{6}$$

where $S_i(s,t)$, for any $1 \leq i \leq n$, represents the service process of the i^{th} server.

C. MGF-based Probabilistic Bounds

Deterministic network calculus [38] can provide worst-case upper bounds on the backlog and the delay if traffic envelopes (an upper bound on the arrival process) as well as a service curve (a lower bound on the service process) are considered. However, when analyzing systems with random input and/or service (like wireless networks), due to a possibly non-trivial probability for the service increment or arrival increment to be zero, the worst-case analysis is no longer useful to describe the performance any more. In such cases, probabilistic performance bounds provide more useful and realistic description of the system performance than worst-case analysis. In the probabilistic setting (where the arrival process A and/or the service process S are stationary random processes), the backlog and delay bounds defined in (2) and (3) respectively are reformulated in a stochastic sense as:

$$\mathbb{P}\left(B(t) > b^{\varepsilon'}\right) \leq \varepsilon' \text{ and } \mathbb{P}\left(W(t) > w^{\varepsilon''}\right) \leq \varepsilon'', \tag{7}$$

where $b^{\varepsilon'}$ and $w^{\varepsilon''}$ denote the target probabilistic backlog and delay associated with violation probabilities ε' and ε'' respectively. These performance bounds can be obtained by the distributions of the processes, i.e., in terms of the arrival and service processes MGFs [22] or their Mellin transforms [34]. These approaches constitute what we refer to as stochastic network calculus and they are most suitable for the analysis of wireless networks.

In general, the MGF-based bounds are obtained by applying Chernoff's bound, that is, given a random variable X, we have

$$\mathbb{P}(X \geq x) \leq e^{-\theta x}\mathbb{E}\left[e^{\theta X}\right] = e^{-\theta x}\mathbb{M}_X(\theta),$$

whenever the expectation exists, where $\mathbb{E}[Y]$ and $\mathbb{M}_Y(\theta)$ denote the expectation and the moment generating function (or the Laplace transform) of Y, respectively, and θ is an arbitrary non-negative free parameter. Given the stochastic process $X(s,t), t \geq s$, we define the MGF of X for any $\theta \geq 0$ as [40]

$$\mathbb{M}_X(\theta,s,t) \triangleq \mathbb{E}\left[e^{\theta X(s,t)}\right].$$

Moreover, $\overline{\mathbb{M}}_X(\theta,s,t) \triangleq \mathbb{M}_X(-\theta,s,t) = \mathbb{E}\left[e^{-\theta X(s,t)}\right]$ is also defined in a similar way.

A number of properties of MGF-based network calculus are summarized in [40]. In this work, we consider a queuing system comprised of a set of tandem queues. Using (6), the MGF of the end-to-end service process, written as $\overline{\mathbb{M}}_{S_{\text{net}}}(\theta,s,t)$, of N tandem queues with service processes $S_i, i = 1,\ldots N$, is bounded by

$$\begin{aligned}
&\overline{\mathbb{M}}_{S_{\text{net}}}(\theta,s,t) \triangleq \overline{\mathbb{M}}_{S_1 \otimes S_2 \otimes \cdots \otimes S_N}(\theta,s,t) \\
=&\mathbb{E}\left[\exp\left(-\theta \cdot \inf_{s \leq u_1 \leq \cdots \leq u_{N-1} \leq t}\left\{\sum_{i=1}^{N} S_i(u_{i-1},u_i)\right\}\right)\right] \\
\leq &\sum_{s \leq u_1 \leq \cdots \leq u_{N-1} \leq t} \prod_{i=1}^{N} \overline{\mathbb{M}}_{S_i}(\theta,u_{i-1},u_i),
\end{aligned} \tag{8}$$

where $u_0 = s$ and $u_N = t$, and (8) is obtained via applying the union bound and independence assumption. In addition, we denote the MGF of the arrival process by $\mathbb{M}_A(\theta,s,t)$. Then, probabilistic backlog and delay bounds satisfying (7) above, can be respectively expressed by [40], [41]

$$b^{\varepsilon'} = \inf_{\theta>0}\left\{\frac{1}{\theta}\left(\log \mathsf{M}(\theta,t,t) - \log \varepsilon'\right)\right\}, \tag{9}$$

and

$$w^{\varepsilon''} = \inf\left\{w : \inf_{\theta>0}\left\{\mathsf{M}(\theta,t+w,t)\right\} \leq \varepsilon''\right\}, \tag{10}$$

where $\mathsf{M}(\theta,s,t)$ is given as

$$\mathsf{M}(\theta,s,t) \triangleq \sum_{u=0}^{\min(s,t)} \mathbb{M}_A(\theta,u,t) \cdot \overline{\mathbb{M}}_{S_{\text{net}}}(\theta,u,s). \tag{11}$$

Note that, $\mathsf{M}(\theta,s,t)$ is only valid when the arrival and service processes are independent. Also, we can see that, $\mathsf{M}(\theta,s,t)$ given by (11) is the key to derive the probabilistic backlog and delay bounds.

III. Performance Analysis of MmWave Multi-Hop Wireless Network

A. System Model

We consider a multi-hop wireless network in mmWave bands, as shown in Fig. 2, consisting of a source S, n ($n \geq 1$) full-duplex relays R_i, $i = 1,2,\ldots,n$ and a destination D. For simplifying illustration, we assign the labels 0, 1, …, $n+1$

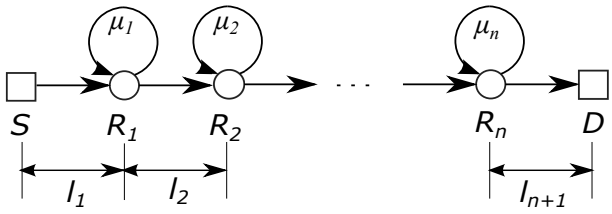

Fig. 2. A multi-hop wireless network with n full-duplex relays.

to the ordered nodes. That is, S and D correspond to nodes 0 and $(n+1)$, respectively. Furthermore, we label the channel between nodes $(i-1)$ and i as the i^{th} hop in the set of hops $\mathcal{I}_{\mathcal{H}}$, i.e., $i \in \mathcal{I}_{\mathcal{H}} = \{1, 2, \ldots, n+1\}$, and the distance between the two nodes by l_i (in meter). We denote the channel gain coefficient of the i^{th} hop by g_i. Given the separation distance l_i, a generalized model of g_i (in dB) for the mmWave channel is given by [42], [43]

$$g_i[\text{dB}] = -\left(\alpha + 10\beta \log_{10}(l_i) + \xi_i\right), \tag{12}$$

where α and β are the least square fits of floating intercept and slope of the best fit, and $\xi_i \sim \mathcal{N}(0, \sigma_i^2)$ corresponds to the log-normal shadowing effect with variance σ_i^2. The values of the parameters α and β greatly depend on the environment configurations. Our service characterization and performance analysis are carried out in terms of these two parameters in order to incorporate all such configurations.

In addition to the (large scale) fading effect, without loss of generality, the proposed model also considers the self-interference at each full-duplex relay node. Compared to self-interference, the interference impact from other neighboring nodes is small, due to the rapid attenuation of the millimeter waves, and thus it is ignored. A common approach to model the self-interference is to use a coefficient $0 \leq \mu \leq 1$ that characterizes the coupling between the transmitter and the receiver of a full-duplex device. It has been shown that the self-interference is linearly related the transmission power [14]. In the presence of self-interference, the signal to interference plus noise ratio (SINR) in the i^{th} hop, denoted by γ_i, for the described channel is expressed as

$$\gamma_i = \kappa \cdot \omega_i \cdot g_i\,, \quad s.t., \quad \omega_i = \begin{cases} \dfrac{\lambda_{i-1}}{1+\mu_i\lambda_i}, & i \in \{1, 2, \ldots, n\} \\ \lambda_{i-1}, & i = n+1 \end{cases}, \tag{13}$$

where κ is a scalar depending on system configuration, i.e., the antenna gains of the communication pair, g_i is the channel gain coefficient given by (12), $\lambda_i \triangleq \frac{P_i}{N_0}$ denotes the transmitted signal-to-noise ratio (SNR) at node i corresponding to transmit power P_i and background noise power N_0.

For the multi-hop scenario, we assume the stochastic process of each hop to be stationary and independent in time. That is, we can use a series of independent random variables γ_i to characterize the multi-hop channels, namely, $\gamma_i^{(k)} \overset{\ell}{=} \gamma_i$ in all time slot k, where $\overset{\ell}{=}$ denotes equality in law (i.e., in distribution). The shadowing effect, which is due to objects obstructing the propagation of mmWave radios, is considered in the channel gain coefficient model given by (12). Regarding the stochastic behavior of different links, generally, shadowing is not spatially independent. Considering the fact that highly directional antennas are commonly used for mmWave communications, it is safe to assume that the obstructions of radio propagation behave independently, which justifies the independence assumption across hops.

In general, the fading distributions of the subsequent channels in multi-hop wireless network may not be identical. Nevertheless, it is worthwhile to decompose the set of hops into subsets of hops with identically distributed channel gains. More precisely, we decompose the set of hops, $\mathcal{I}_{\mathcal{H}}$, into m subsets, $\mathcal{X}_k, k \in \mathcal{I}_{\mathcal{M}} = \{1, \ldots, m\}$, where, $\mathcal{I}_{\mathcal{H}} = \bigcup_{k=1}^{m} \mathcal{X}_k$, with $\mathcal{X}_i \bigcap \mathcal{X}_j = \emptyset$ for all $i, j \in \mathcal{I}_{\mathcal{M}}$ such that $i \neq j$, where $\mathcal{X}_k$ is defined as the set of indices such that

$$\mathcal{X}_k = \{j \in \mathcal{I}_{\mathcal{H}}, k \in \mathcal{I}_{\mathcal{M}} : F_{\gamma_j}(x) = F^{\langle k \rangle}(x)\}, \tag{14}$$

where $F_X(x)$ is the probability distribution function of the random variable X, $F^{\langle k \rangle}(x)$ represents a unique distribution function corresponding to the subset of i.i.d. hops denoted by the index $k \in \mathcal{I}_{\mathcal{M}}$. We emphasize that $|\mathcal{I}_{\mathcal{H}}| \geq |\mathcal{I}_{\mathcal{M}}|$, where $|\mathcal{Y}|$ represents the cardinality of the set $\mathcal{Y}$, and the equality is attained when the multi-hop network is fully heterogeneous. In such extreme case, each subset $\mathcal{X}_k$ contains only one element, i.e., the channel at each hop has a distinct fading distribution.

To address the transmit power allocation problem for the multi-hop network, we consider a system with sum power P_{tot} constraint, i.e., $\sum_{i=0}^{n} P_i = P_{\text{tot}}$. Equivalently, given a constant background noise power N_0 for all hops, the sum power constraint can be reformulated as

$$\sum_{i=0}^{n} \lambda_i = \lambda_{\text{tot}} \triangleq \frac{P_{\text{tot}}}{N_0}. \tag{15}$$

B. MGF Bound for the Cumulative Service Process

The performance bounds given by (9) and (10) require the computation of MGFs of arrival and service processes. For the arrival process, we consider in this work the $(\sigma(\theta), \rho(\theta))$ traffic characterization with parameters $\sigma(\theta) = \delta_b$ and $\rho(\theta) = \rho_a$, i.e., we assume deterministically bounded arrival process [25], [37]. That is, in the statistical sense, for any stochastic arrival processes, there always exist proper deterministic asymptotic arrival rate ρ_a and burst parameter δ_b, such the MGF of arrival processes, denoted by $\mathbb{M}_A(\theta, s, t)$, is upper bounded by

$$\mathbb{M}_A(\theta, s, t) \leq e^{\theta(\rho_a(t-s)+\delta_b)} \triangleq e^{\theta\delta_b} \left(p_a(\theta)\right)^{t-s}, \tag{16}$$

for any $\theta > 0$, where $p_a(\theta) = e^{\theta\rho_a}$.

Regarding the service process, we present in the following a series of results that apply to a Shannon-capacity type service process. Given a channel SINR γ, in this model the service process (in bit per second) of the channel is given by

$$C(\gamma) = \eta \ln(1+\gamma),$$

where $\eta = \frac{W}{\ln 2}$ with channel bandwidth W. By (1), the cumulative service process for hop i, $S_i(s,t)$, is given by

$$S_i(s,t) = \sum_{k=s}^{t-1} C(\gamma_i(k)) = \eta \sum_{k=s}^{t-1} \ln\left(1+\gamma_i(k)\right), \tag{17}$$

where $\gamma_i(k)$ is the instantaneous SINR in the k^{th} time slot for the i^{th} hop given in terms of g_i in (12) and ω_i in (13).

However, associated with the specific fading characteristic of mmWave channels, an exact expression for the MGF of this Shannon-type cumulative service process in (17) is intractable, since the *shifted log-normal random variable*, i.e., $(1+\gamma_i(k))$, has no closed-form inverse moment. Instead, in the following lemma, we present an upper bound on the MGF of such Shannon-type service processes $S_i(s,t)$.

Lemma 1. *Let $F_X(x)$ denote the cumulative distribution function (c.d.f.) of a non-negative random variable X, for any $\delta > 0$ and $\theta \geq 0$ we have*

$$\mathbb{E}\left[(1+X)^{-\theta}\right] \leq \mathcal{U}_{\delta,X}(\theta),$$

where

$$\mathcal{U}_{\delta,X}(\theta) = \min_{u\geq 0}\left\{(1+\delta N_\delta(u))^{-\theta} + \sum_{k=1}^{N_\delta(u)} a_{\theta,\delta}(k) F_X(k\delta)\right\},$$

where $N_\delta(u)$ and $a_{\theta,\delta}(k)$ are respectively given by $N_\delta(u) = \lfloor \frac{u}{\delta} \rfloor$ and $a_{\theta,\delta}(k) = (1+(k-1)\delta)^{-\theta} - (1+k\delta)^{-\theta}$.

For the proof of Lemma 1, please refer to [36]. Note that the tightness of the bound obtained in Lemma 1 depends on the parameter δ, the discretization step size. Technically, a smaller step size yields a tighter upper bound while leading to higher computational costs.

Based on Lemma 1, a bound on the MGF of the service process for any single-server wireless system with service process increments given by the Shannon capacity is given:

Theorem 1. *Given $S(s,t) = \eta \sum_{k=s}^{t-1} \ln(1+\gamma(k))$ with independent positive $\gamma(k)$, an upper bound on $\overline{\mathbb{M}}_S(\theta,s,t)$ is given by*

$$\overline{\mathbb{M}}_S(\theta,s,t) \leq \prod_{k=s}^{t-1} q(\theta,k),$$

where $q(\theta,k) = \mathcal{U}_{\delta,\gamma(k)}(\eta\theta)$. Furthermore, if $\gamma(k) \overset{\ell}{=} \gamma$ holds for all k, then $q(\theta,k) = q(\theta)$ and the above expression reduces to $\overline{\mathbb{M}}_S(\theta,s,t) \leq (q(\theta))^{t-s}$.

Proof: Starting from the definition of $\overline{\mathbb{M}}_S(\theta,s,t)$ and using the independence assumption of $\gamma(k)$ in k, we have

$$\begin{aligned}\overline{\mathbb{M}}_S(\theta,s,t) &= \mathbb{E}\left[\exp\left(-\theta\cdot S(s,t)\right)\right]\\ &= \mathbb{E}\left[\prod_{k=s}^{t-1}\exp\left(-\theta\eta\ln(1+\gamma(k))\right)\right] = \prod_{k=s}^{t-1}\mathbb{E}\left[(1+\gamma(k))^{-\theta\eta}\right].\end{aligned}$$

Applying Lemma 1 to the right hand side of the expression above, Theorem 1 immediately follows. ∎

Next, we provide a MGF bound on the network service for multi-hop wireless networks with heterogeneous, independent Shannon-type service processes per link. The channel categorization, shown in (14), is used for expression simplifications.

Theorem 2. *The network service process $S_{\text{net}}(s,t)$ of a multi-hop wireless network consisting of n relays and characterized by the decomposable set of hops $\mathcal{I}_{\mathcal{H}} = \bigcup_{i=1}^{m}\mathcal{X}_i$ following* (14)*, where the subset $\mathcal{X}_i$ is associated with the randomly varying SINR $\hat{\gamma}_i$ and has a Shannon-type service process increment $\ln(1+\gamma)$, has the following MGF bound*

$$\overline{\mathbb{M}}_{S_{\text{net}}}(\theta,s,t) \leq \sum_{\sum_{i=1}^{m}\pi_i = t-s}\prod_{i=1}^{m}\binom{\pi_i+|\mathcal{X}_i|-1}{|\mathcal{X}_i|-1}\hat{q}_i^{\pi_i}(\theta), \quad (18)$$

where $\hat{q}_i(\theta) = \mathcal{U}_{\delta,\hat{\gamma}_i}(\eta\theta)$ for all $i \in \mathcal{I}_{\mathcal{M}}$.

Proof: Using equation (6) and (8), we can bound the MGF for the $n+1$ hops network service process by

$$\begin{aligned}\overline{\mathbb{M}}_{S_{\text{net}}}(\theta,s,t) &\leq \sum_{s=\tau_1\leq\cdots\leq\tau_{n+1}=t}\prod_{i=1}^{n+1}\overline{\mathbb{M}}_{S_i}(\theta,\tau_{i-1},\tau_i)\\ &\leq \sum_{\sum_{i=1}^{n+1}\tau_i = t-s} q_1^{\tau_1}(\theta)q_2^{\tau_2}(\theta)\cdots q_{n+1}^{\tau_{n+1}}(\theta)\\ &= \sum_{\sum_{i=1}^{m}\pi_i = t-s}\prod_{i=1}^{m}\hat{q}_i^{\pi_i}(\theta)\sum_{\sum_{k\in\mathcal{X}_i}\tau_k=\pi_i} 1\end{aligned}$$

where the first inequality is obtained by using (8), and the second inequality is obtained by using the change of variables $\tau_i = \tau_i - \tau_{i-1}$ and the stationarity of the service processes, i.e., $\overline{\mathbb{M}}_{S_i}(\theta,\tau_{i-1},\tau_i) = \overline{\mathbb{M}}_{S_i}(\theta,\tau_i-\tau_{i-1})$, then applying Theorem 1. The equality in the last line is obtained by aggregating similar terms, i.e., $\pi_i = \sum_{k\in\mathcal{X}_i}\tau_k$. Applying the combinations of multi-sets theory [44], it is known that

$$\sum_{\sum_{k\in\mathcal{X}_i}\tau_k=\pi_i} 1 = \binom{\pi_i+|\mathcal{X}_i|-1}{|\mathcal{X}_i|-1},$$

where $|\mathcal{X}_i|$ denotes the cardinality of $\mathcal{X}_i$, and then the theorem is concluded. ∎

We emphasize that, all results presented so far apply to general cases of distributions of link SINR γ. Thus, the results have wide applicability to wireless (and wired) network analysis, as long as Shannon-type service processes are assumed.

C. Probabilistic Performance Bounds

The general probabilistic total backlog and end-to-end delay bounds for a multi-hop wireless network are given by (9) and (10), respectively. Both bounds are given in terms of $\mathsf{M}(\theta,s,t)$ in (11). Theorem 3 provides an upper bound on the function $\mathsf{M}(\theta,s,t)$, and hence, probabilistic performance bounds for multi-hop wireless networks, when the arrival is characterized by (16) and the network service is provided by Theorem 2.

Let us first define $\mathcal{K}_{\tau,n,m}(x)$ as

$$\begin{aligned}\mathcal{K}_{\tau,n,m}(x) \triangleq & x^{\tau}\cdot\binom{n+1-m+\tau}{n+1-m}\\ &\cdot {}_2F_1(1,n+2-m+\tau;\tau+1;x),\end{aligned}$$

where the *Generalized Hypergeometric Function* ${}_pF_q(\underline{a};\underline{b};x)$, with vectors $\underline{a} = [a_1,\ldots,a_p]$ and $\underline{b} = [b_1,\ldots,b_q]$, is given as

$${}_pF_q(\underline{a};\underline{b};x) \triangleq \sum_{k=0}^{\infty}\left(\frac{\prod_{i=1}^{p}(a_i)_k}{\prod_{j=1}^{q}(b_j)_k}\right)\cdot\frac{x^k}{k!},$$

and $(a_i)_k$ and $(b_i)_k$ are *Pochhammer symbols*.

Theorem 3. *Let m be the number of subsets of identically distributed channels, $\tau \triangleq \max(s-t,0)$, and $V_i(\theta) \triangleq p_a(\theta)\hat{q}_i(\theta)$, a upper bound for $\mathsf{M}(\theta,s,t)$, $\theta > 0$, for the $(n+1)$-hop wireless network is given by*

$$\mathsf{M}(\theta,s,t) \leq \frac{e^{\theta\delta_b}}{p_a^{s-t}(\theta)}\sum_{i=1}^{m}\psi_i(\theta)V_i^{m-1}(\theta)\mathcal{K}_{\tau,n,m}(V_i(\theta)),$$

whenever the stability condition, $\max_{i\in\mathcal{I}_{\mathcal{M}}}\{V_i(\theta)\} < 1$, is satis-

fied. Here, $\psi_i(\theta)$ for all $i \in \{1,\ldots,m\}$ is defined as

$$\psi_i(\theta) \triangleq \begin{cases} \prod_{j\neq i} \left(V_i(\theta)-V_j(\theta)\right)^{-1}, & m \geq 2 \\ 1, & m=1 \end{cases}. \quad (19)$$

Proof: By the definition of $\mathsf{M}(\theta,s,t)$ in (11), we start with the substitution of (16) and (18) in (11), then we have

$$\begin{aligned}&\mathsf{M}(\theta,s,t)\\ \leq& e^{\theta\delta_b}\sum_{u=0}^{\min(s,t)} p_a^{t-u}(\theta)\cdot \sum_{\sum_{i=1}^m \pi_i=s-u}\prod_{i=1}^m \binom{\pi_i+|\mathcal{X}_i|-1}{|\mathcal{X}_i|-1}\hat{q}_i^{\pi_i}(\theta).\end{aligned}$$

Then using the change of variable $u=s-u$ and rearranging terms, we equivalently have

$$\begin{aligned}&\mathsf{M}(\theta,s,t)\\ \leq& \frac{e^{\theta\delta_b}}{p_a^{s-t}(\theta)}\sum_{u=\tau}^{s} p_a^{u}(\theta)\cdot \sum_{\sum_{i=1}^m \pi_i=u}\prod_{i=1}^m \binom{\pi_i+|\mathcal{X}_i|-1}{|\mathcal{X}_i|-1}\hat{q}_i^{\pi_i}(\theta),\end{aligned}$$

Based on above, by splitting the power u for $p_a^u(\theta)$ into components in terms of π_i, we immediately have

$$\begin{aligned}\mathsf{M}(\theta,s,t) \leq& \frac{e^{\theta\delta_b}}{p_a^{s-t}(\theta)}\sum_{u=\tau}^{s}\sum_{\sum_{i=1}^m \pi_i=u}\prod_{i=1}^m \binom{\pi_i+|\mathcal{X}_i|-1}{|\mathcal{X}_i|-1}V_i^{\pi_i}(\theta)\\ \leq& \frac{e^{\theta\delta_b}}{p_a^{s-t}(\theta)}\sum_{u=\tau}^{\infty}\sum_{\sum_{i=1}^m \pi_i=u}\prod_{i=1}^m \binom{\pi_i+|\mathcal{X}_i|-1}{|\mathcal{X}_i|-1}V_i^{\pi_i}(\theta),\end{aligned}$$

where $V_i(\theta) \triangleq p_a(\theta)\hat{q}_i(\theta)$ and $\tau \triangleq \max(s-t,0)$ are respectively defined for notional simplicity, and the last inequality is obtained by pushing s to infinity. Then, we further have

$$\begin{aligned}&\mathsf{M}(\theta,s,t)\\ \leq& \frac{e^{\theta\delta_b}}{p_a^{s-t}(\theta)}\sum_{u=\tau}^{\infty}\binom{u+n+1-m}{n+1-m}\sum_{\sum_{i=1}^m \pi_i=u}\prod_{i=1}^m V_i^{\pi_i}(\theta), \quad (20)\end{aligned}$$

where the following inequality for combinatorics is used, i.e.,

$$\binom{n_1}{k_1}\binom{n_2}{k_2}\cdots\binom{n_M}{k_M} \leq \binom{n_1+n_2+\cdots+n_M}{k_1+k_2+\cdots+k_M}$$

for all $n_i \geq k_i \geq 0$, $i \in \{1,2,\ldots,M\}$.

From (20) on, we need to consider two situations: (i) $m=1$ for the homogeneous network, and (ii) $m \geq 2$, which represents the heterogeneous scenario.

For $m=1$, the expression in (20) directly reduces to

$$\mathsf{M}(\theta,s,t) \leq \frac{e^{\theta\delta_b}}{p_a^{s-t}(\theta)}\sum_{u=\tau}^{\infty}\binom{u+n}{n}V^u(\theta), \quad (21)$$

where $V(\theta)=p_a(\theta)\,\hat{q}(\theta)$, and $\hat{q}(\theta)$ characterizes the homogeneous channel gain.

Regarding $m \geq 2$, the upper bound of $\mathsf{M}(\theta,s,t)$ can be formulated as

$$\begin{aligned}&\mathsf{M}(\theta,s,t)\\ \leq& \frac{e^{\theta\delta_b}}{p_a^{s-t}(\theta)}\sum_{u=\tau}^{\infty}\binom{u+n+1-m}{n+1-m}\sum_{i=1}^m \varphi_i(\theta)V_i^{u+m-1}(\theta) \quad (22)\\ =& \frac{e^{\theta\delta_b}}{p_a^{s-t}(\theta)}\sum_{i=1}^m \varphi_i(\theta)V_i^{m-1}(\theta)\sum_{u=\tau}^{\infty}\binom{u+n+1-m}{n+1-m}V_i^u(\theta),\end{aligned}$$

where $\varphi_i(\theta)=\prod_{j\neq i}\left(V_i(\theta)-V_j(\theta)\right)^{-1}$. Here, the inequality comes from the application of following homogeneous polynomials identity [45], that is,

$$\sum_{k_1+\cdots+k_M=N} x_1^{k_1}x_2^{k_2}\cdots x_M^{k_M} = \sum_{i=1}^{M}\frac{x_i^{N+M-1}}{\prod_{j\neq i}(x_i-x_j)}$$

for any $M \geq 2$ distinct variables, $x_1, x_2, \ldots, x_M$.

Furthermore, we have a closed-form expression in terms of generalized hypergeometric function for the infinite sum [46]

$$\sum_{k=u}^{\infty}\binom{n+k}{k}x^k = x^u\binom{n+u}{u}{}_2F_1(1,n+u+1;u+1;x),$$

whenever $|x|<1$, which subsequently produces the newly defined $\mathcal{K}_{\tau,n,m}(x)$. It is worth noting that, the condition $\max_{i\in\mathcal{I}_{\mathcal{M}}}\{V_i(\theta)\}<1$ should be satisfied, for the sake of stability. Combining (21) and (22) and using (19), then the theorem can be concluded. ∎

In Theorem 3, the stability condition is reduced from the statement that, $V_i(\theta)<1$ should hold for all $1 \leq i \leq m$. From the physical perspective, in the sense of long-term stability, the arrival rate should be less than the service capability on all hops; otherwise, the hop that violates this condition becomes the network bottleneck, thereby producing infinite backlog and delay. The stability condition can be reasoned as follows. If we take the log of both sides of the expression, the condition can be stated as, "the difference between $\log\mathbb{M}_A(\theta,0,t)$ and $-\log\overline{\mathbb{M}}_{S_i}(\theta,0,t)$ is less than 0," i.e., for a given QoS measure θ, the effective capacity (characterized by $-(\theta t)^{-1}\log\overline{\mathbb{M}}_{S_i}(\theta,0,t)$) must be greater than the effective bandwidth (characterized by $(\theta t)^{-1}\log\mathbb{M}_A(\theta,0,t)$), for the same θ, for the system to be stable. This intuitive result was hinted in [25, Ch. 7].

It is evident that, the upper bound of $\mathsf{M}(\theta,s,t)$ by Theorem 3 is suitable for both homogeneous and heterogeneous multi-hop wireless networks. In contrast to the recursive method [35], the classification of hops of the network into m subsets with identical channels, in terms of their channel distributions, provides a straightforward approach to compute $\mathsf{M}(\theta,s,t)$, thereby largely simplifying the obtained expression. From the side of service process each subset of nodes can be considered as homogeneous sub-network, and the overall network service process is given by the $(\min,+)$ convolution of the subnets service processes. It is however worth noting that, although the network service curve expression that we derived is computationally simpler than the recursive expression derived in [35], it involves an additional bounding stage on the MGF of the network service curve which may relax the bound slightly. Given that the computation of such curve

maybe extremely demanding, we feel that such relaxation is warranted. Furthermore, simulation results show that the obtained performance bounds are reasonably tight.

Clearly, the expression provided by Theorem 3 depends on the generalized hypergeometric function, which is computational costly. In what follows, we provide a looser but more simplified upper bound on $\mathsf{M}(\theta,s,t)$ in the homogeneous case specifically, i.e., $m=1$. For that, we first need the following lemma regarding the upper bound on $\mathcal{K}_{\tau,n,1}(x)$.

Lemma 2. *For non-negative integers n and τ, the inequality*

$$\mathcal{K}_{\tau,n,1}(x) \le \mathcal{G}_{\tau,n}(x) \triangleq \min\{\mathcal{G}_1(x), \mathcal{G}_2(x)\}$$

holds for $0 \le x < 1$, where $\mathcal{G}_1(x)$ and $\mathcal{G}_2(x)$ are respectively given by

$$\mathcal{G}_1(x) = \frac{\min\left(1, x^\tau \binom{n+\tau}{n}\right)}{(1-x)^{n+1}}$$

and

$$\mathcal{G}_2(x) = \frac{1}{(1-x)^{n+1}} - \binom{n+\tau}{n+1} x^{\tau-1}.$$

Proof: Note that $\mathcal{K}_{\tau,n,1}(x)$ is explicitly formulated as

$$\mathcal{K}_{\tau,n,1}(x) = \sum_{k=\tau}^{\infty} \binom{n+k}{k} x^k,$$

then the derivation can be performed from the the following two cases:

(i) It is easy to know that, $i+k \le (i+k-\tau)(1+\frac{\tau}{i})$ holds for all $i \ge 1$ and all $k \ge \tau$, then we have

$$\binom{n+k}{k} \le \binom{n+k-\tau}{k-\tau}\binom{n+\tau}{n}.$$

Then we have

$$\mathcal{K}_{\tau,n,1}(x) \le x^\tau \binom{n+\tau}{n} \sum_{k=0}^{\infty} \binom{n+k}{k} x^k, \tag{23}$$

where we used the change of variables, i.e., $k = k-\tau$. It immediately gives $\mathcal{G}_1(x)$ by applying *Newton's Generalized Binomial Theorem* and by taking 1 as the upper limit into account as well.

(ii) On the other hand, it is easy to know that

$$\begin{aligned}\sum_{k=\tau}^{\infty} \binom{n+k}{k} x^k =& \frac{1}{(1-x)^{n+1}} - \sum_{k=0}^{\tau-1} \binom{n+k}{k} x^k \\ \le& \frac{1}{(1-x)^{n+1}} - x^{\tau-1} \sum_{k=0}^{\tau-1} \binom{n+k}{k} \\ =& \frac{1}{(1-x)^{n+1}} - \binom{n+\tau}{n+1} x^{\tau-1},\end{aligned}$$

where inequality is true since $0 \le x < 1$, and the last equality is obtained by applying a combinatorial property [44]. Then $\mathcal{G}_2(x)$ is obtained. ∎

The lemma above allows us to use a simpler expression to describe the upper bound (compared to Theorem 3) on $\mathsf{M}(\theta,s,t)$ for homogeneous networks in particular, and it is shown in the following theorem.

Theorem 4. *For homogeneous $(n+1)$-hop wireless networks characterized by the MGF service bound $\hat{q}(\theta)$, and for any $\theta > 0$, given $p_a(\theta)$ we have*

$$\mathsf{M}(\theta,s,t) \le \frac{e^{\theta\delta_b}}{p_a^{s-t}(\theta)} \cdot \mathcal{G}_{\tau,n}\left(p_a(\theta)\hat{q}(\theta)\right),$$

where $\tau \triangleq \max(s-t,0)$, whenever the stability condition, $p_a(\theta)\hat{q}(\theta) < 1$, holds.

Proof: Applying Lemma 2 in (21) whenever $0 \le p_a(\theta)\hat{q}(\theta) < 1$, then Theorem 4 follows. ∎

Inserting the results from Theorem 3 (or Theorem 4 for merely homogeneous cases), in (9) and (10), we obtain the desired probabilistic bounds on backlog b^ε and delay w^ε in the network, respectively.

IV. Power Allocation for Multi-Hop Networks

In this section, we study optimal power allocation for a mmWave multi-hop network, applying the results presented in the previous section regarding the MGF-based network calculus. For tractability considerations, a sum power constraint is assumed in particular, and the resulting power allocation scheme is optimal for the scenarios with identical shadowing. The cases with per-device power constraint or non-identical shadowing are more complicated, and thus left for our future study. Here, more precisely, we are interested in finding the optimal transmit power allocation of multi-hop network with independent and identically distributed shadowing per hop, $\xi_i, \forall i \in \mathcal{I}_{\mathcal{H}}$, assuming that ξ_i is stationary. In particular, we limit our study to the case of homogenous log-normally distributed shadowing over all links, i.e. we set $\xi_i \overset{\ell}{=} \xi \sim \mathcal{N}(0,\sigma^2)$ for all hops $i \in \mathcal{I}_{\mathcal{H}}$. The case with non-identical shadowing is more involved and is left for future work.

From (9) and (10), it is clearly shown that, probabilistic bounds on the total network backlog and end-to-end delay performance are determined in terms of the function $\mathsf{M}(\theta,s,t)$ defined in (11). This implies that the performance optimization, e.g., with respect to transmit power allocation, of a multi-hop network is equivalent to optimizing the function $\mathsf{M}(\theta,s,t)$, which, with a given arrival process $\mathbb{M}_A$, is equivalent to optimizing $\overline{\mathbb{M}}_{S_{\text{net}}}$. Therefore, in what follows, the optimization subject is the MGF for the network service process, i.e., $\overline{\mathbb{M}}_{S_{\text{net}}}$. Since an exact expression for the MGF of network service process is not attainable, we opt for optimizing a bound on $\overline{\mathbb{M}}_{S_{\text{net}}}$, given by (8), instead. A power allocation that elevates the lower bound on network service capacity corresponds to lower $\overline{\mathbb{M}}_{S_{\text{net}}}$ and thus reduces the probabilistic bounds on network performance.

Theorem 2 provides an upper bound on $\overline{\mathbb{M}}_{S_{\text{net}}}(\theta,s,t)$ and hence a lower bound on the network's service capability [1]. Therefore, in order to maximize the lower bound on the service process, we must minimize the upper bound on $\overline{\mathbb{M}}_{S_{\text{net}}}(\theta,s,t)$. The function $\overline{\mathbb{M}}_{S_{\text{net}}}(\theta,s,t)$ is related to the power allocation

[1]More exactly, a higher server capability is associated with a higher channel capacity of multi-hop network, which therefore gives a smaller $\overline{\mathbb{M}}_{S_{\text{net}}}$, adversely, by the definition of service MGF.

vector $\mathbf{P} \in \mathbb{R}_+^{n+1}$. From (8) we have

$$\overline{\mathbb{M}}_{S_{\rm net}}(\theta,s,t) \leq \sum_{\sum_{i=1}^{n+1}\pi_i=t-s} \prod_{i=1}^{n+1} \left(\mathbb{E}\left[(1+\gamma_i)^{-\theta\eta}\right]\right)^{\pi_i}, \quad (24)$$

where the per node SINR, γ_i, $\forall i \in \mathcal{I}_{\mathcal{H}}$, is given by (17) and is in turn related to the allocated transmit power for the corresponding node. Let $\mathbf{\Xi}_n \subset \mathbb{R}_+^{n+1}$ be the set of feasible power allocation schemes with respect to n intermediate nodes. Furthermore, the sum of all allocated power should be constrained by the total power budget, i.e.,

$$P_{\sum} \triangleq \sum_{i\in\mathcal{I}_{\mathcal{H}}} P_i \leq P_{\rm tot},$$

where $P_{\rm tot}$ is the total power budget. For any power allocation $\mathbf{P} \triangleq \{P_i\}_{i\in\mathcal{I}_{\mathcal{H}}} \in \mathbf{\Xi}_n$, we define $\mathbf{P}$ as a *feasible* power allocation scheme if the power constraint above is satisfied.

To determine the optimal power allocation strategy, we need the following two lemmas first. To be more precise, in Lemma 3 below, we show that, given a feasible power allocation, the maximal network service capability is achieved only when the SINRs for all hops are identically distributed. Next, in Lemma 4 we show the existence and uniqueness of the optimal power allocation vector $\mathbf{P}^*$ when $P_{\sum} = P_{\rm tot}$.

Lemma 3 (Sufficiency)**.** *Given the sum transmit power budget $P_{\rm tot}$ for a $(n+1)$-hop wireless network, a feasible power allocation $\mathbf{P}^*$, where $P_{\sum} = P_{\rm tot}$, that results in identically distributed SINR over all hops maximizes the lower bound on network service process whenever such $\mathbf{P}^*$ exists.*

Proof: Note that the network service process is characterized by its MGF bound, $\overline{\mathbb{M}}_{S_{\rm net}}(\theta,s,t), s>0$. Furthermore, a lower bound on the service process corresponds to an upper bound on $\overline{\mathbb{M}}_{S_{\rm net}}(\theta,s,t)$, which is given by (24). Since $P_{\sum} = P_{\rm tot}$ by assumption, the optimization problem can be formulated as

$$\mathbf{P}^* = \underset{\mathbf{P}:P_{\sum}=P_{\rm tot}}{\operatorname{argmin}} \sum_{\sum_{i=1}^{n+1}\pi_i=t-s} \prod_{i=1}^{n+1} \left(\mathbb{E}\left[(1+\gamma_i)^{-\theta\eta}\right]\right)^{\pi_i}. \quad (25)$$

To prove the lemma, we use the *generalized Haber inequality* [47]. That is, for any m non-negative real numbers $x_1, x_2, \ldots, x_m$, and for all $n \geq 0$, we have

$$\sum_{i_1+\cdots+i_m=n} \prod_{k=1}^{m} x_i^{i_k} \geq \binom{n+m-1}{m-1} \left(\frac{1}{m}\sum_{k=1}^{m} x_k\right)^n.$$

The above holds with equality *if and only if* $x_i = x_j$ for any $1 \leq i,j \leq m$. Using this result, the minimum in (25) can be achieved by choosing a power allocation vector $\mathbf{P}^*$ such that

$$\mathbb{E}\left[(1+\gamma_i)^{-\theta\eta}\right] = \mathbb{E}\left[(1+\gamma_j)^{-\theta\eta}\right]$$

for all $i,j \in \mathcal{I}_{\mathcal{M}}$, which equivalently indicates that the SINRs are identically distributed across all $n+1$ hops, i.e., $\gamma_j \overset{d}{=} \gamma_i$, for all $i \in \mathcal{I}_{\mathcal{H}}$. The resulting MGF service bound under $\mathbf{P}^*$ power allocation is then given by

$$\begin{aligned}\overline{\mathbb{M}}^*_{S_{\rm net}}(\theta,s,t) \leq& \binom{t-s+n}{n} \left(\frac{1}{n+1}\sum_{i=1}^{n+1}\mathbb{E}\left[(1+\gamma_i)^{-\theta\eta}\right]\right)^{t-s} \\ =& \binom{t-s+n}{n} \left(\mathbb{E}\left[(1+\hat{\gamma})^{-\theta\eta}\right]\right)^{t-s}. \end{aligned} \quad (26)$$

The first step is obtained by applying the generalized Haber inequality, with *strict equality* under optimal power allocation, to (24). The last step follows since $\gamma_i, \forall i \in \mathcal{I}_{\mathcal{H}}$ are i.i.d. under optimal power allocation, and the fact that a random variable is uniquely determined by its MGF, and by letting $\hat{\gamma} \overset{d}{=} \gamma_i$. ■

Lemma 3 shows that the key enabler of optimal multi-hop network operation is the maintenance of identically distributed channels' SINR across all hops. Note that this result applies to arbitrary networks where the service process is characterized by a Shannon-type link model, as long as the individual links are not coupled in terms of interference (only self-interference is considered). In contrast, in what follows we present an approach for allocating transmit power [2] to achieve identically distributed SINR in a mmWave multi-hop network. Given a background noise power of N_0, we define $\lambda_i = \frac{P_i}{N_0}$. Due to the one-to-one correspondence of λ_i and P_i and for convenience we opt to work with λ_i for the derivations that follows.

For γ_i, $i \in \mathcal{I}_{\mathcal{H}}$, we use

$$\gamma_i = \kappa \cdot 10^{-0.1\alpha}\omega_i l_i^{-\beta} \cdot 10^{-0.1\xi_i}$$

to rewrite (13). Note that the shadowing effects are assumed to be homogeneous and log-normally distributed over all hops, i.e., $\xi_i \sim \mathcal{N}(0,\sigma^2)$, where the log-normal shadowing variance σ^2 is independent of the transmit power, since $\omega_i l_i^{-\beta}$ depends on the power allocated to transmitter i, then a power allocation scheme that enables the equality $\omega_i l_i^{-\beta} = \omega_j l_j^{-\beta}$ for any $i,j \in \mathcal{I}_{\mathcal{H}}$ is sufficient to ensure identically distributed SINR $\gamma_i, \forall i$.

We follow an iterative approach starting from the last hop of the network, i.e., the $(n+1)^{\rm th}$ hop, and moving backwards. Assume that $\omega_i l_i^{-\beta} = c$ holds for any $i \in \mathcal{I}_{\mathcal{H}}$, where c is a constant. Let $i = n+1$, then according to (13), $\omega_{n+1} = \lambda_n$ and therefore, $\lambda_n = c \cdot l_{n+1}^{\beta}$. Similarly, for $i = n$, we obtain

$$\lambda_{n-1} = (1+\mu_n\lambda_n)\cdot c \cdot l_n^{\beta} = c \cdot l_n^{\beta} + c^2\mu_n \left(l_n l_{n+1}\right)^{\beta}.$$

Then by recursively applying $\lambda_{i-1} = (1+\mu_i\lambda_i)\cdot c \cdot l_i^{\beta}$, for all $i \in \mathcal{I}_{\mathcal{H}}$, and after some manipulation we obtain

$$\lambda_i = \sum_{k=1}^{n-i+1} c^k \left(\mu_{i+k}^{-1}\prod_{u=1}^{k}\mu_{i+u}\cdot l_{i+u}^{\beta}\right) \triangleq \sum_{k=1}^{n-i+1}\nu_{i,k}\cdot c^k \quad (27)$$

for all $0 \leq i \leq n$.

With the constraint $P_{\sum} \leq P_{\rm tot}$, which corresponds to $\lambda_{\sum} \triangleq \frac{P_{\sum}}{N_0} \leq \frac{P_{\rm tot}}{N_0} \triangleq \lambda_{\rm tot}$, we can obtain the value of c using Lemma 3 and by solving the equation $\lambda_{\sum} = \lambda_{\rm tot}$ subject to

$$\lambda_{\sum} = \sum_{i=0}^{n}\left(\sum_{k=1}^{n-i+1}\nu_{i,k}c^k\right) = \sum_{k=1}^{n+1}\left(\sum_{i=0}^{n+1-k}\nu_{i,k}\right)\cdot c^k, \quad (28)$$

where the last equality is obtained by collecting terms con-

[2]The power is assumed to be infinitely divisible during the power allocation.

taining c^k for $1 \leq k \leq n+1$. Then $\hat{\gamma}$ can be expressed as

$$\hat{\gamma} = \kappa \cdot 10^{-0.1(\alpha+\xi)} \cdot c. \tag{29}$$

Lemma 4 (Existence)**.** *Given a $(n+1)$-hop wireless network operating under transmit power budget P_{tot}, there always exists a unique optimal power allocation $\mathbf{P}^*$ such that $P_{\sum} = P_{\text{tot}}$, among all feasible $\mathbf{P} \in \mathbf{\Xi}_n$ in terms of maximizing a lower bound on network service process.*

Proof: The proof consists of two parts: (i) the existence and uniqueness of the power allocation scheme given $P_{\sum} = P_{\text{tot}}$, and (ii) the optimality. The notations in derivations below follow the fashion we used previously.

(i) To show that there is exactly one real root c that meets the constraint on λ_{tot}, we first construct $f(x)$ as follows

$$f(x) \triangleq \sum_{k=1}^{n+1} \left(\sum_{i=0}^{n+1-k} \nu_{i,k} \right) x^k - \lambda_{\text{tot}}. \tag{30}$$

Due to the facts that $f(0) = -\lambda_{\text{tot}} < 0$ and $f(+\infty) = +\infty$, since $f(x)$ is continuous, by the *Intermediate Value Theorem*, there is a positive c such that $f(c) = 0$, which means that equation $f(x) = 0$ has a root. Furthermore, to prove the uniqueness of the root, we assume equation $f(x) = 0$ has at least two positive roots x_1 and x_2. Suppose that $x_1 < x_2$ such that $f(x_1) = f(x_2) = 0$. Note that $f(x)$ is continuous on the closed interval $[x_1, x_2]$ and differentiable on the open interval (x_1, x_2), it is easy to find that the three hypotheses of *Rolle's Theorem* are simultaneously satisfied. Thus, there should be a number $x^* \in (x_1, x_2)$ such that $f'(x^*) = 0$. However,

$$f'(x) = \sum_{k=1}^{n+1} \left(\sum_{i=0}^{n+1-k} \nu_{i,k} \right) k x^{k-1} > 0$$

holds for any point $x \in (0, +\infty)$, which contradicts the initial assumption and hence we conclude that $x_1 = x_2$ which proves the uniqueness of the root for the equation $f(x) = 0$ and hence the uniqueness of the optimal power control vector.

(ii) To prove the optimality of $\mathbf{P}^*$, we assume that the optimal solution is obtained with the sum power $P'_{\sum}$ that relates to the power allocation vector $\mathbf{P}'$, where $P'_{\sum} < P^*_{\sum} = P_{\text{tot}}$. In other words, we can obtain $\hat{\gamma}'$ associated with $\mathbf{P}'$, such that

$$\mathbb{E}\left[(1+\hat{\gamma}')^{-\theta\eta}\right] \leq \mathbb{E}\left[(1+\hat{\gamma}^*)^{-\theta\eta}\right], \tag{31}$$

where $\hat{\gamma}^*$ similarly relates to $\mathbf{P}^*$. For notational simplicity, by using (29), we define

$$g(c) \triangleq \mathbb{E}\left[(1+\hat{\gamma})^{-\theta\eta}\right] = \mathbb{E}\left[(1+\kappa 10^{-0.1(\alpha+\xi)}c)^{-\theta\eta}\right].$$

Let us consider all possible power allocation schemes $\mathbf{P}$ such that $P_{\sum} \leq P_{\text{tot}}$. It is evident that, the derivative of $g(c)$ over $P_{\sum}$ gives

$$\begin{aligned} \frac{dg(c)}{dP_{\sum}} &= g'(c) \cdot \frac{dc}{dP_{\sum}} = g'(c) \cdot \left(\frac{dP_{\sum}}{dc}\right)^{-1} \\ &= -\theta\eta \cdot \mathbb{E}\left[\frac{\kappa 10^{-0.1(\alpha+\xi)}}{\left(1+\kappa 10^{-0.1(\alpha+\xi)}c\right)^{1+\theta\eta}}\right] \cdot \frac{N_0}{f'(c)} < 0. \end{aligned} \tag{32}$$

which indicates that $g(c)$ monotonically decreases in $P_{\sum}$. Since c is uniquely determined by $P_{\sum}$ as shown above and because of (32), we conclude that

$$\mathbb{E}\left[(1+\hat{\gamma}')^{-\theta\eta}\right] > \mathbb{E}\left[(1+\hat{\gamma}^*)^{-\theta\eta}\right],$$

which contradicts the initial assumption in (31). Thus, the optimal solution is achieved only when $P_{\sum} = P_{\text{tot}}$ is satisfied, which completes the proof. ■

Lemma 3 shows that allocating power in such a way that it results in i.i.d. SINRs across the hops is optimal, while Lemma 4 states that utilizing all the available power for transmission is optimal since it provides the best network performance. The intuition behind these results is that avoiding bottleneck is the best strategy, while utilizing more power for transmission enhances network performance. Furthermore, Lemma 3 and Lemma 4 provide the minimization on the MGF bound of the service process rather than minimizing the actual process. Nevertheless, such minimization results in maximizing the lower bound on network service which in turn enables the computation of better network backlog and end-to-end delay bounds and more efficient resource allocation and network dimensioning when based on the computed results. In light of the above, we have the following theorem to show the exact power allocations.

Theorem 5. *Given the total power budget P_{tot}, i.e., $P_{\sum} \leq P_{\text{tot}}$, and the background noise power N_0, for the mmWave channel described in* (12)*, and let x^* denote the positive solution for the algebraic equation*

$$\sum_{k=1}^{n+1} \left(\sum_{i=0}^{n+1-k} \nu_{i,k} \right) x^k = \frac{P_{\text{tot}}}{N_0},$$

with $\nu_{i,k}$ given by

$$\nu_{i,k} = \mu_{i+k}^{-1} \cdot \prod_{u=1}^{k} \mu_{i+u} \cdot l_{i+u}^{\beta},$$

where μ_i and l_i are the model parameters defined in Sec. III, then, there exists a unique optimal power allocation strategy $\mathbf{P}^* \in \mathbf{\Xi}_n$, such that

$$P_i^* = N_0 \sum_{k=1}^{n-i+1} \nu_{i,k} \cdot (x^*)^k, \quad \textit{for } i \in \mathcal{I}_{\mathcal{H}}.$$

Proof: Using Lemmas 3 and 4, the theorem immediately follows by applying the mapping between the transmit power and the SINR, i.e., $P_{\text{tot}} = \lambda_{\text{tot}} N_0$ and $P_i = \lambda_i N_0$. ■

V. Self-interference Impact in MmWave Networks

To investigate the impact of self-interference on network performance, we consider a particular case, where the separation distances between adjacent nodes are assumed to be equal to l, e.g., $l_i = l$ for $\forall i \in \mathcal{I}_{\mathcal{H}}$, and all relays have an identical self-interference coefficient μ. Closed-form expressions for the network performance can be obtained under these assumptions which provide more insights to the network operation.

In the following analysis, we assume that the optimal power allocation scheme proposed in Theorem 5 is used. Under this power allocation, we have $c = \omega_i l_i^{-\beta}$ for $\forall i \in \mathcal{I}_{\mathcal{H}}$. Note that c

in this case is a measure of the SINR of channels, and hence it directly influences the network performance. (13) shows that, the parameter ω_i, and therefore the function c, are functions of μ. Therefore, in this section we represent this measure by the function $c(\mu) = \omega_i(\mu) l_i^{-\beta}$. Applying (28) under the proposed power allocation scheme as well as the conditions $P_{\sum} = P_{\text{tot}}$ and $\mu_i = \mu$, the optimal λ_i in (27), denoted by λ_i^*, reduces to

$$\begin{aligned}\lambda_i^* &= \mu^{-1} \sum_{k=1}^{n-i+1} \left(c(\mu)\mu l^{\beta}\right)^k \\ &= \begin{cases} c(\mu) l^{\beta} \cdot \dfrac{\left(c(\mu)\mu l^{\beta}\right)^{n-i+1} - 1}{c(\mu)\mu l^{\beta} - 1}, & \text{if } c(\mu)\mu l^{\beta} \neq 1 \\ \dfrac{2\lambda_{\text{tot}}(n-i+1)}{(n+1)(n+2)}, & \text{otherwise.} \end{cases}\end{aligned} \tag{33}$$

In the above, we used the geometric sum to obtain the first case. It is easy to find that, the case $c(\mu)\mu l^{\beta} = 1$ corresponds to a particular situation for the self-interference coefficient μ, i.e., $\mu = (2\lambda_{\text{tot}})^{-1}(n+1)(n+2)$, which immediately gives the optimal $c(\mu)$ as $c(\mu) = 2\lambda_{\text{tot}}\left[(n+1)(n+2) l^{\beta}\right]$ by applying $c(\mu) = \left(\mu l^{\beta}\right)^{-1}$. It is worth noting that, $c(\mu)\mu l^{\beta} = 1$ here corresponds to a very special case that rarely occurs in realistic scenarios, since μ, which is only related to the relay implementation, is independent from λ_{tot} and n. In this sense, for most cases $\mu = (2\lambda_{\text{tot}})^{-1}(n+1)(n+2)$ is not satisfied. Therefore, from the perspective of generality, our interest mainly focuses on the case $c(\mu)\mu l^{\beta} \neq 1$.

According to the assumption of optimal power allocation that gives $P_{\sum} = P_{\text{tot}}$ according to Lemma 4, we have

$$\begin{aligned}\lambda_{\text{tot}} &= \sum_{i=0}^{n} \lambda_i^* = \frac{c(\mu) l^{\beta}}{c(\mu)\mu l^{\beta} - 1} \sum_{i=0}^{n} \left(\left(c(\mu)\mu l^{\beta}\right)^{n-i+1} - 1\right) \\ &= \frac{c(\mu) l^{\beta}}{c(\mu)\mu l^{\beta} - 1} \left(c(\mu)\mu l^{\beta} \frac{\left(c(\mu)\mu l^{\beta}\right)^{n+1} - 1}{c(\mu)\mu l^{\beta} - 1} - n - 1\right),\end{aligned} \tag{34}$$

where we use the change of variables $j = n - i + 1$ and then apply the geometric sum formula in the last step.

For notational simplicity, we set $t = c(\mu)\mu l^{\beta}$ with $t \neq 1$, then (34) can be written as

$$\mu\lambda_{\text{tot}} = \frac{t}{t-1}\left(t \cdot \frac{t^{n+1} - 1}{t - 1} - (n+1)\right),$$

which subsequently gives

$$t^{n+3} - (n + 2 + \mu\lambda_{\text{tot}}) t^2 + (n + 1 + 2\mu\lambda_{\text{tot}}) t = \mu\lambda_{\text{tot}}. \tag{35}$$

Recovering t to $c(\mu)\mu l^{\beta}$ and dividing both sides of (35) by μ, in terms of $c(\mu)$, we immediately obtain

$$a_1(\mu) c^{n+3}(\mu) + a_2(\mu) c^2(\mu) + a_3(\mu) c(\mu) - \lambda_{\text{tot}} = 0, \tag{36}$$

where $a_i(\mu)$, $i = 1, 2, 3$ are respectively given by

$$\begin{cases} a_1(\mu) = \mu^{n+2} l^{(n+3)\beta}, \\ a_2(\mu) = -(n + 2 + \mu\lambda_{\text{tot}})\mu l^{2\beta}, \\ a_3(\mu) = (n + 1 + 2\mu\lambda_{\text{tot}}) l^{\beta}. \end{cases}$$

To this end, the *Descartes' Sign Rule* [48] can be applied to determine the number of positive roots of (36). The rule states that, when the terms in a polynomial are ordered according to their variable exponent, then the number of positive real roots of that polynomial is either the number of sign changes, say n, between consecutive non-zero coefficients, or is less than that by an even number, i.e., $n, n-2, n-4, \ldots$. Clearly, (36) has one or three real positive root(s), if there exist real positive solutions. In addition, we can see that, there are two repeated positive roots $c_1(\mu) = c_2(\mu) = \left(\mu l^{\beta}\right)^{-1}$. By excluding the two repeated roots that violate the condition $c(\mu)\mu l^{\beta} \neq 1$, we are left with one unique positive solution $c(\mu) \neq \left(\mu l^{\beta}\right)^{-1}$ for (36), under optimal power allocation, which coincides with the claim in Lemma 4.

For the arbitrary positive integer n, there is no explicit generic analytical solution of (36) for $c(\mu)$. Hence, in order to keep track of $c(\mu)$ with respect to μ, we compute the first derivative over μ on both sides of (36), then we have

$$\begin{aligned}0 =& a_1'(\mu) c^{n+3}(\mu) + (n+3) a_1(\mu) c^{n+2}(\mu) c'(\mu) \\ &+ a_2'(\mu) c^2(\mu) + 2 a_2(\mu) c(\mu) c'(\mu) \\ &+ a_3'(\mu) c(\mu) + a_3(\mu) c'(\mu),\end{aligned}$$

which gives

$$c'(\mu) = -\frac{a_1'(\mu) c^{n+3}(\mu) + a_2'(\mu) c^2(\mu) + a_3'(\mu) c(\mu)}{(n+3) a_1(\mu) c^{n+2}(\mu) + 2 a_2(\mu) c(\mu) + a_3(\mu)}. \tag{37}$$

The asymptotic behavior of $c(\mu)$ in the two cases, i.e., when $\mu \to 0$ and $n \to \infty$, respectively, is of particular interest, which will be investigated in what follows.

1) For $\mu \to 0$: Note that $c(\mu)$ is bounded by $\frac{\lambda_{\text{tot}}}{(n+1) l^{\beta}}$, since $\sum_1^{n+1} c(\mu) l^{\beta} = \sum_1^{n+1} \omega_i \leq \sum_{i=0}^{n} \lambda_i = \lambda_{\text{tot}}$. Then, (37) can be expressed by

$$\lim_{\mu \to 0} c'(\mu) = \frac{(n+2) l^{2\beta} c^2(\mu) - 2\lambda_{\text{tot}} l^{\beta} c(\mu)}{(n+1) l^{\beta}} \leq 0.$$

In the sense of asymptote, we obtain

$$c(\mu) = \frac{2\lambda_{\text{tot}} l^{-\beta}}{n\left(1 + \exp\left(\frac{2\lambda_{\text{tot}}\mu}{n+1}\right)\right) + 2} \tag{38}$$

by applying the initial condition $c(0) = \frac{\lambda_{\text{tot}}}{(n+1) l^{\beta}}$.

2) For $n \to \infty$: Defining $D \triangleq \mu\lambda_{\text{tot}}$ and $t(\mu) \triangleq c(\mu)\mu l^{\beta}$, the derivative (37) can be written as

$$c'(\mu) = -\frac{c(\mu)}{\mu} \frac{\left(n^2 + (D+3)n + 2\right) t(\mu) - (n+2) D}{\left(n^2 + (D+3)n + 2 + D\right) t(\mu) - (n+3) D}. \tag{39}$$

It is evident that, when λ_{tot} is fixed, $n \to \infty$ yields $n^{-1} D \to 0$. Dividing the numerator and denominator of (39) by n^2, we then have

$$\lim_{n \to \infty} c'(\mu) = -\frac{c(\mu)}{\mu},$$

which immediately gives

$$c(\mu) = K\mu^{-1}, \tag{40}$$

where $K > 0$ is a constant scalar.

Following the notation in (29), we denote by $\hat{\gamma}^*(\mu)$ the SINR with respect to the optimal power allocation proposed by Theorem 5 as a function of self-interference coefficient

μ. Regarding the two asymptotic cases above, we have the following theorem and corollaries to address the relationship between network service capability under optimal power allocation and the self-interference coefficient.

Theorem 6. *Assuming the optimal power allocation in Theorem 5, in the two extreme cases discussed above, the maximized lower bound of network service capability decreases as μ grows.*

Proof: Recalling that the lower bound of network service capability is characterized by $\mathbb{E}\left[(1+\hat{\gamma}^*(\mu))^{-\theta\eta}\right]$, we can see that

$$\frac{d}{d\mu}\mathbb{E}\left[(1+\hat{\gamma}^*(\mu))^{-\theta\eta}\right] = \frac{d}{dc(\mu)}\mathbb{E}\left[(1+\hat{\gamma}^*(\mu))^{-\theta\eta}\right]c'(\mu)$$
$$= -\theta\eta\cdot\mathbb{E}\left[\frac{\kappa 10^{-0.1(\alpha+\xi)}}{\left(1+\kappa c(\mu)10^{-0.1(\alpha+\xi)}\right)^{1+\theta\eta}}\right]\cdot c'(\mu)$$
$$= -\theta\eta\cdot\mathbb{E}\left[\frac{\hat{\gamma}^*(\mu)}{(1+\hat{\gamma}^*(\mu))^{1+\theta\eta}}\right]\cdot\frac{c'(\mu)}{c(\mu)} > 0,$$

since it has been shown that $c'(\mu) < 0$ for asymptotic situations, e.g., when $\mu \to 0$, which corresponds to case that μ is extremely small, or $n \to \infty$, which corresponds to the case that n is sufficiently large. This indicates $\mathbb{E}\left[(1+\hat{\gamma}^*(\mu))^{-\theta\eta}\right]$ monotonically increases with μ, which equivalently shows the degradation of the maximized lower bound of network service capability. Thus, the theorem is concluded. ■

VI. Numerical Results and Discussion

In this section, we provide numerical results for the total backlog and end-to-end delay bounds for mmWave multi-hop wireless network discussed in Sec. III and validate them by simulations. Moreover, in the presence of self-interference, the performance of optimal power allocation presented in Sec. IV and V is demonstrated and further discussed.

Here, in particular, the 60 GHz band (ranging from 57 GHz to 64 GHz) is selected for our mmWave multi-hop network, and the common system parameters, including the parameters specifically associated with 60 GHz channels, are summarized in Table I. In addition, we assume the following regarding the network configuration:

- Deterministic arrivals with a constant rate ρ_a, and a burst $\delta_b = 0$;
- All relays have identical μ, and are uniformly deployed along the path from source to destination;
- Sufficiently large (or infinite) buffer size at each relay, i.e., overflow effects are neglected;
- A time-slotted system with time intervals of 1 second are assumed.

Under this scenario, we investigate the following:

1) We first validate the derived upper bounds for probabilistic end-to-end delay and total backlog from Theorem 3.
2) Secondly, based on the validated bounds, we investigate the impact of optimal power control, self-interference and relay density on the probabilistic performance of mmWave multi-hop networks.

TABLE I
System Parameters

Parameters	Symbol	Value
Bandwidth	W	500 MHz
Antenna Gain Scalar	κ	70 dBi
Power Budget	P_{tot}	50 Watt
Noise Power Density	N_0/W	-114 dBm/MHz
Hop Length	l	0.5 km
Path Loss Intercept	α	70
Path Loss Slope	β	2.45
STD of Shadowing	σ	8 dB

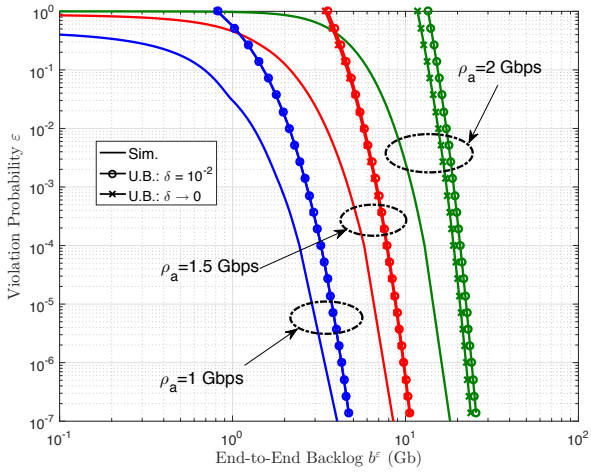

Fig. 3. Violation probability ε v.s. targeted theoretical backlog bounds b^{ε}, compared to simulations for different $\rho_a = 1$, 1.5 and 2 Gbps, with $n = 10$, and $\delta = 10^{-2}$ and $\delta \to 0$, respectively.

For the sake of simplicity, in what follows the analytical bounds for homogeneous scenarios are all illustrated by Theorem 4, while heterogeneous counterparts are provided by applying Theorem 3.

A. Bound Validation

We start with considering a tandem 60 Ghz network consisting of $n = 10$ relays that have identical self-interference coefficient $\mu = -80$ dB. From Table I and the power constraint formulated in the form of (15), we determine $\lambda_{\text{tot}} = 134$ dB. Figs. 3 and 4 show the total backlog and the end-to-end delay bounds respectively, compared to their corresponding simulated values. Recall that the SINR distributions are identical per hop due to applying the optimal power allocation policy from Theorem 5, resulting in $m = 1$ of Theorem 3.

In Fig. 3, given a violation probability ε, we observe that the simulated total backlog (the curve without marker) rises as the arrival rate increases from 1 Gbps to 2 Gbps due to an increasing utilization of the system. Clearly, the simulated violation probability of backlog asymptotically approaches the analytical upper bound (the curve with marker) as the target

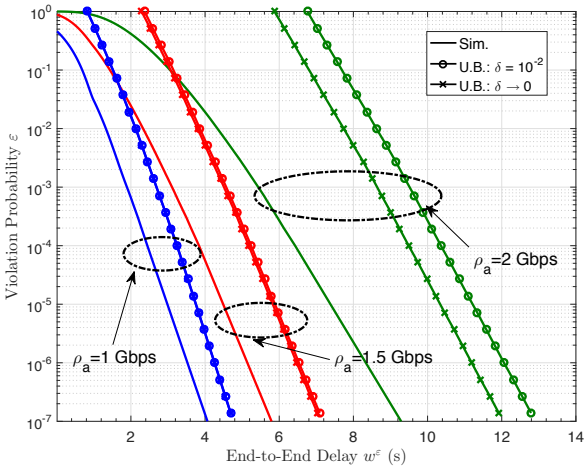

Fig. 4. Violation probability ε v.s. targeted theoretical delay bounds w^ε, compared to simulations for different $\rho_a = 1$, 1.5 and 2 Gbps, with $n = 10$, and $\delta = 10^{-2}$ and $\delta \to 0$, respectively.

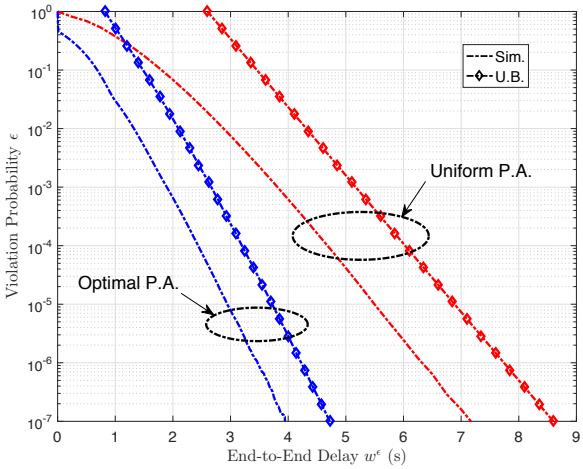

Fig. 5. Violation probability ε v.s. targeted theoretical delay bounds w^ε, compared to simulations for two power allocation strategies, with $n = 10$, $\rho_a = 1$ Gbps and $\delta = 10^{-2}$.

end-to-end backlog b^ε increases. The plot furthermore contains the information on the accuracy of bound provided by Lemma 1, as we compare in the plot the corresponding analytical bounds for a granularity of $\delta = 10^{-2}$ as well as for letting $\delta \to 0$. We observe that the two curves are quite close together, which confirms also our findings in [36] that the MGF bound provided by Lemma 1 is close to the true MGF of the service process for reasonable granularities δ. The only exception occurs for the end-to-end delay violation probability with a higher traffic load of $\rho_a = 2$ Gbps, indicating that the step size might be required to be adapted in certain scenarios. In addition, regarding the end-to-end delay w^ε with respect to the violation probability ε in Fig. 4, we find that the end-to-end delay is not linearly dependent on the arrival rate, while the delay violation probability bound becomes less accurate as the the utilization approaches the saturation point [3]. This is due to the fact that, we use a parameterized bound to characterize the $\overline{\mathbb{M}}_{S_{\text{net}}}$, the discretization errors introduced by the parameterized bound will get enlarged, since the feasible set of θ to meet the stability condition correspondingly shrinks. Therefore, the precision decays. Despite this, asymptotically the simulated system behavior and the the bounds show the same slope, concluding our validations for derived bounds.

B. Impact of Optimal Power Allocation

Fig. 5 demonstrates the merit of adopting the optimal power allocation, with respect to its impact on the end-to-end delay. We consider a network that consists of $n = 10$ relays, the self-interference coefficient is $\mu = -80$ dB, and the arrival rate is fixed to $\rho_a = 1$ Gbps. We use a uniformly allocated powers $\{P_i\}_{i=0}^n = \frac{50}{11}$W as a baseline for comparison. From the figure, it is evident that, the upper bound associated with the optimal power allocation (referring to Theorem 4 for the homogeneous

[3]The "saturation point" can be understood as the maximum ρ_a such that $\max_{i\in\mathcal{I}_\mathcal{M}}\{V_i\} = 1$, which reflects the upper limit of network without yielding infinite backlog and delay.

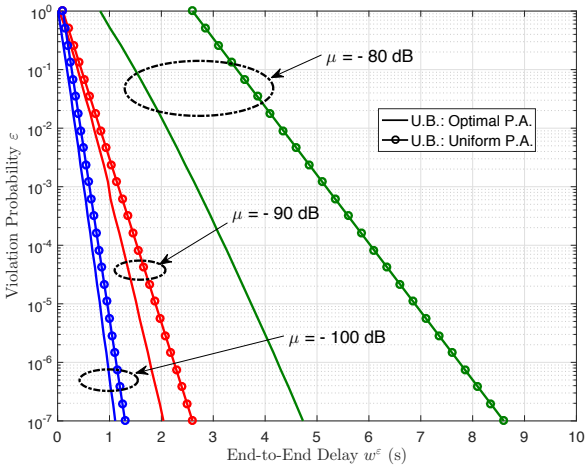

Fig. 6. Violation probability ε v.s. targeted theoretical delay bounds w^ε, for two power allocation strategies, with $\mu = -80$ dB, -90 dB and -100 dB, respectively, where $n = 10$, $\rho_a = 1$ Gbps, and $\delta = 10^{-2}$.

case) is asymptotically tight, while its counterpart (here applying the result for $m \geq 2$ in Theorem 3, since the non-optimal power allocation yields the heterogeneity) is not. The slackness of bounds for the heterogeneous scenario comes from producing the binomial coefficient of (20) in Theorem 3, where the upper bound is generalized in a simplified and unified manner. In other words, compared to the recursive approach by [35], the tightness of our proposed method is sacrificed for gaining a lower computational complexity for the heterogeneous cases. Fortunately, the asymptotic tightness can be guaranteed for both homogeneous and heterogeneous scenarios, and this allows us to keep track of realistic performance behaviors. Furthermore, under a sum power constraint, we can see that, the network performance without the optimal power allocation suffers severe degradation, in terms of the end-to-end delay. It is evident that, the bound performance degradation is also significantly exacerbated as μ grows, e.g., comparing e.g., the

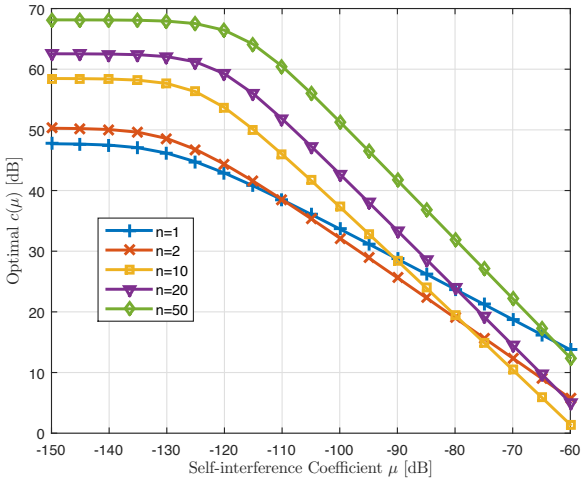

Fig. 7. $c(\mu)$ v.s. μ for different relay densities characterized by $n = 1$, 2, 10, 20 and 50, respectively, with $L = 5$ km, $P_{\text{tot}} = 50$ W.

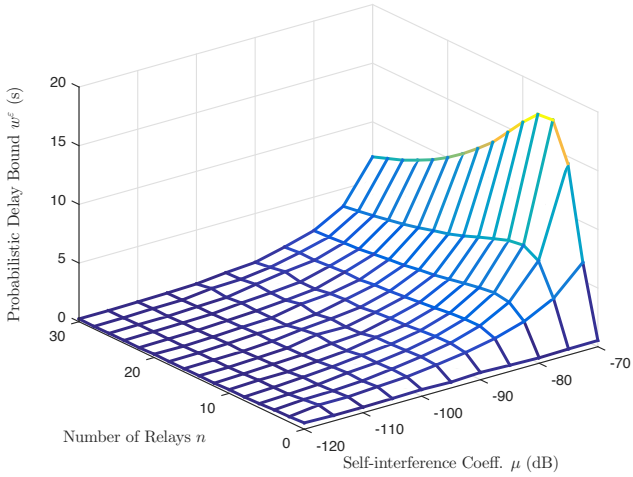

Fig. 8. Probabilistic delay bound w^{ε} v.s. n and μ jointly, with $\varepsilon = 10^{-6}$.

gap between optimal and uniform power allocations schemes with $\mu = -80$ dB and that with $\mu = -100$ dB. This obvious deterioration indicates the great importance of adopting the optimal power allocation by Theorem 5, especially when the self-interference is significantly greater than the noise, i.e., the interference-limited system.

Given different self-interference coefficients, i.e., $\mu = -100$ dB, -90 dB and -80 dB, in Fig. 6, we furthermore investigate the impact of self-interference on the network performance bound through the optimal power allocation. Clearly, in the situation $\mu = -80$ dB, the optimal power allocation scheme enables a remarkable improvement in terms of performance bounds, while this benefit diminishes when μ decreases, as shown from the gaps for $\mu = -90$ dB and $\mu = -100$ dB. Despite the slackness of upper bound for the heterogeneous cases (with respect to the observations from Fig. 5), we are still able to conclude that the optimal power allocation is more important in case of high interference coupling, or low SINR scenarios, in general.

C. Impacts of Self-Interference and Relay Density

In the following, we further investigate the performance of 60 GHz networks operated by optima power allocation while varying the self-interference coupling coefficient μ. Here, the separation distance between source and destination is fixed to $L = 5$ km, and an arbitrary number of relays with a sum power constraint is uniformly placed between the source and destination nodes. As we deploy more relays, the separation distance between adjacent nodes decreases as $l = \frac{L}{n+1}$.

From Lemma 3, we know that the SINR per link, determined by $c(\mu) = \omega^*(\mu) l^{-\beta}$, yields the service performance, where $\omega^*(\mu)$ denotes the optimal $\omega_i(\mu)$ for $\forall i \in \mathcal{I}_{\mathcal{H}}$ obtained by applying the optimal power allocation. We study hence the impact of μ on $c(\mu)$ by this relation, rather than straightforwardly to aim at the probabilistic backlog and delay violation probability bounds. The behavior of $c(\mu)$ with respect to the varying self-interference coefficient μ for different relay densities is shown in Fig. 7. For all curves, there exists a "waterfall" tendency with regard to $c(\mu)$ as μ increases, i.e., dividing the curve into a "flat" and "falling" stages, respectively. We find that, the point from which on this transition happens depends on the node density n. Taking the scenario $n = 50$ as an example, more precisely, when μ is below $\mu_c \approx -120$ dB, $c(\mu)$ remains flat by increasing μ. Keeping on elevating μ, however, $c(\mu)$ will encounter a dramatical decay once μ exceeds μ_c. This behavior relates to the fact that, the system switches from a noise-limited one to an interference-limited one as μ grows, such that the self-interference becomes the dominant factor restricting the level of $c(\mu)$. We also observe that, generally speaking, a higher relay density will result in a higher $c(\mu)$. However, when the self-interference coefficient is significant and the system being limited by interference, i.e., $\mu \geq -90$ dB, a sparser relay deployment is surprisingly able to provide a higher $c(\mu)$. From Fig. 7, we summarize that despite improving $c(\mu)$ by means of increasing n, the overall performance improves only if μ relates not to a strongly interference-limited system. Hence, optimizing the network performance by changing the node density must take the self-interference coefficient into account, since higher relay densities do not always imply higher performance.

In Fig. 8, the probabilistic end-to-end delay bound w^{ε} with respect to a varying self-interference coefficient μ and a varying number of relays n is further demonstrated. For more noise-limited systems, the delay bound is barely sensitive to different number of relays (in fact a higher number of relays has a beneficial impact on the delay bound, which is not significantly visible in this plot), while for strongly interference-limited systems, e.g., when $\mu = -70$ dB, either a low or a higher number of relays outperforms relay densities in between significantly. Recall that as the node density increases, the link distances get shorter while the transmit power per relay also decreases. Still, as the results for noise-limited systems demonstrate, the resulting SINR improves as the relay density increases if the self-interference coefficient is

small. When the self-interference coefficient increases, the performance degrades as long as the emitted transmit power per relay creates a *significant* self-interference with the own receiver. This happens precisely for medium number of relays, while for a larger relay density, the resulting self-interference per node drops below the noise level (asymptotically), thereby leading to a better system performance.

VII. Conclusions

We investigate stochastic performance guarantees, i.e., the probabilistic end-to-end backlog and delay, for mmWave multi-hop wireless networks with full-duplex buffered relays, by means of MGF-based stochastic network calculus. According to specific propagation features of mmWave radios, a cumulative service process characterization with self-interference is proposed, in terms of the MGF of its channel capacity. Based on this characterization, probabilistic upper bounds associated with overall network performance are developed. In addition, we propose an optimal power allocation scheme in the presence of self-interference, aiming at enhancing the network performance. The analytical framework of this paper supports a broad class of multi-hop networks, in terms of homogeneous and heterogeneous, where the asymptotic tightness of computed upper bounds has been validated. Results reveal that, the self-interference coefficient plays a crucial role in improving network performance. Another interesting and important finding is that, given the sum power constraint, increasing the relay density does not always improve network performance unless the self-interference coefficient is sufficiently small. We believe that approaches developed in this paper will have a variety of applications in designing and optimizing networks for next generation wireless communications, in terms of performance guarantees and enhancements.

References

[1] T. S. Rappaport, S. Sun, R. Mayzus, H. Zhao, Y. Azar, K. Wang, G. N. Wong, J. K. Schulz, M. Samimi, and F. Gutierrez, "Millimeter wave mobile communications for 5G cellular: It will work!" *IEEE Access*, vol. 1, pp. 335–349, 2013.

[2] R. C. Daniels and R. W. Heath, "60 GHz wireless communications: emerging requirements and design recommendations," *IEEE Vehicular Technology Magazine*, vol. 2, no. 3, pp. 41–50, 2007.

[3] N. Guo, R. C. Qiu, S. S. Mo, and K. Takahashi, "60-GHz millimeter-wave radio: Principle, technology, and new results," *EURASIP Journal on Wireless Communications and Networking*, vol. 2007, no. 1, pp. 48–48, 2007.

[4] N. Moraitis and P. Constantinou, "Measurements and characterization of wideband indoor radio channel at 60 GHz," *IEEE Transactions on Wireless Communications*, vol. 5, no. 4, pp. 880–889, 2006.

[5] P. F. Smulders, "Statistical characterization of 60-GHz indoor radio channels," *IEEE Transactions on Antennas and Propagation*, vol. 57, no. 10, pp. 2820–2829, 2009.

[6] S. Geng, J. Kivinen, X. Zhao, and P. Vainikainen, "Millimeter-wave propagation channel characterization for short-range wireless communications," *IEEE Transactions on Vehicular Technology*, vol. 58, no. 1, pp. 3–13, 2009.

[7] J. Reig, M.-T. Martínez-Inglés, L. Rubio, V.-M. Rodrigo-Peñarrocha, and J.-M. Molina-García-Pardo, "Fading Evaluation in the 60 GHz Band in Line-of-Sight Conditions," *International Journal of Antennas and Propagation*, vol. 2014, 2014.

[8] G. Yang, J. Du, and M. Xiao, "Maximum Throughput Path Selection With Random Blockage for Indoor 60 GHz Relay Networks," *IEEE Transactions on Communications*, vol. 63, no. 10, pp. 3511–3524, 2015.

[9] E. J. Violette, R. H. Espeland, R. O. DeBOLT, and F. Schwering, "Millimeter-wave propagation at street level in an urban environment," *IEEE Transactions on Geoscience and Remote Sensing*, vol. 26, no. 3, pp. 368–380, 1988.

[10] E. Ben-Dor, T. S. Rappaport, Y. Qiao, and S. J. Lauffenburger, "Millimeter-wave 60 GHz outdoor and vehicle AOA propagation measurements using a broadband channel sounder," in *IEEE Global Telecommunications Conference (GLOBECOM2011)*. IEEE, 2011, pp. 1–6.

[11] M. R. Akdeniz, Y. Liu, M. K. Samimi, S. Sun, S. Rangan, T. S. Rappaport, and E. Erkip, "Millimeter wave channel modeling and cellular capacity evaluation," *IEEE Journal on Selected Areas in Communications*, vol. 32, no. 6, pp. 1164–1179, 2014.

[12] M. Williamson, G. Athanasiadou, and A. Nix, "Investigating the effects of antenna directivity on wireless indoor communication at 60 GHz," in *The 8th IEEE International Symposium on Personal, Indoor and Mobile Radio Communications (PIMRC97)*, vol. 2. IEEE, 1997, pp. 635–639.

[13] A. Sahai, G. Patel, and A. Sabharwal, "Pushing the limits of full-duplex: Design and real-time implementation," *arXiv preprint arXiv:1107.0607*, 2011.

[14] M. Duarte and A. Sabharwal, "Full-duplex wireless communications using off-the-shelf radios: Feasibility and first results," in *Conference Record of the Forty Fourth Asilomar Conference on Signals, Systems and Computers (ASILOMAR2010)*. IEEE, 2010, pp. 1558–1562.

[15] M. Jain, J. I. Choi, T. Kim, D. Bharadia, S. Seth, K. Srinivasan, P. Levis, S. Katti, and P. Sinha, "Practical, real-time, full duplex wireless," in *Proceedings of the 17th annual international conference on Mobile computing and networking*. ACM, 2011, pp. 301–312.

[16] L. Li, K. Josiam, and R. Taori, "Feasibility study on full-duplex wireless millimeter-wave systems," in *2014 IEEE International Conference on Acoustics, Speech and Signal Processing (ICASSP)*. IEEE, 2014, pp. 2769–2773.

[17] V. V. Mai, J. Kim, S.-W. Jeon, S. W. Choi, B. Seo, and W.-Y. Shin, "Degrees of freedom of millimeter wave full-duplex systems with partial CSIT," *IEEE Communications Letters*, vol. 20, no. 5, pp. 1042–1045, 2016.

[18] Z. Wei, X. Zhu, S. Sun, Y. Huang, A. Al-Tahmeesschi, and Y. Jiang, "Energy-Efficiency of Millimeter-Wave Full-Duplex Relaying Systems: Challenges and Solutions," *IEEE Access*, vol. 4, pp. 4848–4860, 2016.

[19] H. Abbas and K. Hamdi, "Full duplex relay in millimeter wave backhaul links," in *2016 IEEE Wireless Communications and Networking Conference (WCNC)*. IEEE, 2016, pp. 1–6.

[20] T. Dinc, A. Chakrabarti, and H. Krishnaswamy, "A 60 GHz CMOS full-duplex transceiver and link with polarization-based antenna and RF cancellation," *IEEE journal of solid-state circuits*, vol. 51, no. 5, pp. 1125–1140, 2016.

[21] Z. Wei, X. Zhu, S. Sun, and Y. Huang, "Energy-Efficiency-Oriented Cross-Layer Resource Allocation for Multiuser Full-Duplex Decode-and-Forward Indoor Relay Systems at 60 GHz," *IEEE Journal on Selected Areas in Communications*, vol. 34, no. 12, pp. 3366–3379, 2016.

[22] M. Fidler, "Survey of deterministic and stochastic service curve models in the network calculus," *IEEE Communications Surveys & Tutorials*, vol. 12, no. 1, pp. 59–86, 2010.

[23] R. L. Cruz, "A calculus for network delay. I. Network elements in isolation," *IEEE Transactions on Information Theory*, vol. 37, no. 1, pp. 114–131, 1991.

[24] R. Cruz, "A calculus for network delay. II. Network analysis," *IEEE Transactions on Information Theory*, vol. 37, no. 1, pp. 132–141, Jan 1991.

[25] C.-S. Chang, *Performance guarantees in communication networks*. Springer, 2000.

[26] C.-S. Chang, Y.-m. Chiu, and W. T. Song, "On the performance of multiplexing independent regulated inputs," in *ACM SIGMETRICS Performance Evaluation Review*, vol. 29, no. 1. ACM, 2001, pp. 184–193.

[27] C. Li, A. Burchard, and J. Liebeherr, "A network calculus with effective bandwidth," *IEEE/ACM Transactions on Networking (TON)*, vol. 15, no. 6, pp. 1442–1453, 2007.

[28] M. Fidler, "A Network Calculus Approach to Probabilistic Quality of Service Analysis of Fading Channels," in *IEEE Global Telecommunications Conference (GLOBECOM '06)*, Nov 2006, pp. 1–6.

[29] K. Mahmood, A. Rizk, and Y. Jiang, "On the Flow-Level Delay of a Spatial Multiplexing MIMO Wireless Channel," in *Proc. of IEEE ICC Communications QoS, Reliability and Modeling Symposium, 2011, Japan*, 2011.

[30] M. Rao, F. J. Lopez-Martinez, M.-S. Alouini, and A. Goldsmith, "MGF approach to the analysis of generalized two-ray fading models," *IEEE*

Transactions on Wireless Communications, vol. 14, no. 5, pp. 2548–2561, 2015.

[31] H. Tabassum, Z. Dawy, E. Hossain, and M.-S. Alouini, "Interference statistics and capacity analysis for uplink transmission in two-tier small cell networks: A geometric probability approach," *IEEE Transactions on Wireless Communications*, vol. 13, no. 7, pp. 3837–3852, 2014.

[32] M.-S. Alouini and M. K. Simon, "An MGF-based performance analysis of generalized selection combining over Rayleigh fading channels," *IEEE Transactions on Communications*, vol. 48, no. 3, pp. 401–415, 2000.

[33] F. Yilmaz and M.-S. Alouini, "A unified MGF-based capacity analysis of diversity combiners over generalized fading channels," *IEEE Transactions on Communications*, vol. 60, no. 3, pp. 862–875, 2012.

[34] H. Al-Zubaidy, J. Liebeherr, and A. Burchard, "Network-Layer Performance Analysis of Multihop Fading Channels," *IEEE/ACM Transactions on Networking*, vol. 24, no. 1, pp. 204–217, Feb 2016.

[35] N. Petreska, H. Al-Zubaidy, R. Knorr, and J. Gross, "On the recursive nature of end-to-end delay bound for heterogeneous wireless networks," in *2015 IEEE International Conference on Communications (ICC),*, June 2015, pp. 5998–6004.

[36] G. Yang, M. Xiao, J. Gross, H. Al-Zubaidy, and Y. Huang, "Delay and Backlog Analysis for 60 GHz Wireless Networks," in *2016 IEEE Global Communications Conference (GLOBECOM)*, Dec 2016, pp. 1–7.

[37] C.-S. Chang, "Stability, queue length, and delay of deterministic and stochastic queueing networks," *IEEE Transactions on Automatic Control*, vol. 39, no. 5, pp. 913–931, 1994.

[38] J.-Y. Le Boudec and P. Thiran, *Network calculus: a theory of deterministic queuing systems for the internet*. Springer, 2001, vol. 2050.

[39] Y. Jiang and Y. Liu, *Stochastic network calculus*. Springer, 2008, vol. 1.

[40] M. Fidler, "An end-to-end probabilistic network calculus with moment generating functions," in *14th IEEE International Workshop on Quality of Service (IWQoS2006)*. IEEE, 2006, pp. 261–270.

[41] H. Al-Zubaidy, J. Liebeherr, and A. Burchard, "A (min,$\times$) network calculus for multi-hop fading channels," in *IEEE Proceedings (INFOCOM2013)*. IEEE, 2013, pp. 1833–1841.

[42] S. Rangan, T. Rappaport, and E. Erkip, "Millimeter-Wave Cellular Wireless Networks: Potentials and Challenges," *Proceedings of the IEEE*, vol. 102, no. 3, pp. 366–385, March 2014.

[43] T. S. Rappaport, G. R. Maccartney, M. K. Samimi, and S. Sun, "Wideband millimeter-wave propagation measurements and channel models for future wireless communication system design," *IEEE Transactions on Communications*, vol. 63, no. 9, pp. 3029–3056, 2015.

[44] R. A. Brualdi, *Introductory combinatorics*. New York, 1992.

[45] H. Belbachir and F. Bencherif, "Linear recurrent sequences and powers of a square matrix," *Integers*, vol. 6, p. A12, 2006.

[46] WolframAlpha, computational knowledge engine. Wolfram Alpha LLC. [Online]. Available: http://www.wolfram.com

[47] H. Belbachir and A. ALGER, "A multinomial extension of an inequality of Haber," *J. Ineq. Pure Appl. Math*, vol. 9, no. 4, 2008.

[48] B. Anderson, J. Jackson, and M. Sitharam, "Descartes' rule of signs revisited," *American Mathematical Monthly*, pp. 447–451, 1998.